Paleozoic to early Cenozoic cooling and exhumation of the basement underlying the eastern Puna plateau margin prior to plateau growth

N. Insel,[1,2] M. Grove,[3] M. Haschke,[4] J. B. Barnes,[5] A. K. Schmitt,[6] and M. R. Strecker[1]

Received 11 June 2012; revised 18 October 2012; accepted 26 October 2012; published 22 December 2012.

[1] Constraining the pre-Neogene history of the Puna plateau is crucial for establishing the initial conditions that attended the early stage evolution of the southern extent of the Andean plateau. We apply high- to low-temperature thermochronology data from plutonic rocks in northwestern Argentina to quantify the Paleozoic, Mesozoic and early Tertiary cooling history of the Andean crust. U-Pb crystallization ages of zircons indicate that pluton intrusion occurred during the early mid-Ordovician (490–470 Ma) and the late Jurassic (160–150 Ma). Lower-temperature cooling histories from $^{40}Ar/^{39}Ar$ analyses of K-feldspar vary substantially. Basement rocks underlying the western Puna resided at temperatures below 200°C (<6 km depth) since the Devonian (~400 Ma). In contrast, basement rocks underlying the southeastern Puna were hotter (~200–300°C) throughout the Paleozoic and Jurassic and cooled to temperatures of <200°C by ~120 Ma. The southeastern Puna basement records a rapid cooling phase coeval with active extension of the Cretaceous Salta rift at ~160–100 Ma that we associate with tectonic faulting and lithospheric thinning. The northeastern Puna experienced protracted cooling until the late Cretaceous with temperatures <200°C during the Paleocene. Higher cooling rates between 78 and 55 Ma are associated with thermal subsidence during the postrift stage of the Salta rift and/or shortening-related flexural subsidence. Accelerated cooling and deformation during the Eocene was focused within a narrow zone along the eastern Puna/Eastern Cordillera transition that coincides with Paleozoic/Mesozoic structural and thermal boundaries. Our results constrain regional erosion-induced cooling throughout the Cenozoic to have been less than ~150°C, which implies total Cenozoic denudation of <6–4 km.

Citation: Insel, N., M. Grove, M. Haschke, J. B. Barnes, A. K. Schmitt, and M. R. Strecker (2012), Paleozoic to early Cenozoic cooling and exhumation of the basement underlying the eastern Puna plateau margin prior to plateau growth, *Tectonics*, *31*, TC6006, doi:10.1029/2012TC003168.

1. Introduction

[2] Orogenic plateaus are some of the most prominent and enigmatic features on Earth [e.g., *Isacks*, 1988; *Fielding et al.*, 1994; *Royden*, 1996; *Allmendinger et al.*, 1997; *Hatzfeld and Molnar*, 2010; *Schildgen et al.*, 2012]. One of the least constrained, yet crucial parameters required for understanding orogenic plateau development is the thermal and mechanical state of the crust both prior to and during the earliest phases of plateau formation [*Vanderhaeghe*, 2012]. Previous studies in the central Andes have argued that the onset, spatial pattern, and style of lithospheric deformation was controlled by lithospheric strength and temperature [*Whitman et al.*, 1996; *Babeyko and Sobolev*, 2005] as well as preexisting crustal heterogeneities [e.g., *Allmendinger et al.*, 1983; *Grier et al.*, 1991; *Allmendinger et al.*, 1997; *Kley et al.*, 1999; *Carrera et al.*, 2006; *Oncken et al.*, 2006; *Hongn et al.*, 2007]. In particular, lithospheric weakening through magmatism and shortening is considered to have been a controlling factor for explaining variations in Altiplano-Puna plateau deformation during the early to mid-Cenozoic [*Isacks*, 1988; *Wdowinski and Bock*, 1994]. Changes in Cenozoic exhumation rates have been documented throughout the central Andes [e.g., *Elger et al.*, 2005; *Ege et al.*, 2007; *Carrapa and DeCelles*, 2008;

[1]Department of Earth and Environmental Sciences, Potsdam University, Potsdam, Germany.
[2]Now at Department of the Geophysical Sciences, University of Chicago, Chicago, Illinois, USA.
[3]Department of Geological and Environmental Sciences, Stanford University, California, USA.
[4]Umwelt- und Ingenieurtechnik GmbH Dresden, Dresden, Germany.
[5]Department of Geological Sciences, University of North Carolina at Chapel Hill, Chapel Hill, North Carolina, USA.
[6]Department of Earth and Space Sciences, University of California, Los Angeles, California, USA.

Corresponding author: N. Insel, Department of the Geophysical Sciences, University of Chicago, 5734 S. Ellis Ave., Chicago, IL 60637, USA. (nadinsel@uchicago.edu)

0278-7407/12/2012TC003168

Carrapa et al., 2009], but it is less well known if these periods were spatially synchronous across the plateau region or if they followed a more disparate pattern in time and space. An even more fundamental question is the extent to which Cenozoic deformation, exhumation, and the creation of topography were influenced by the magnitude, location, and timing of pre-Cenozoic thermal processes and denudation.

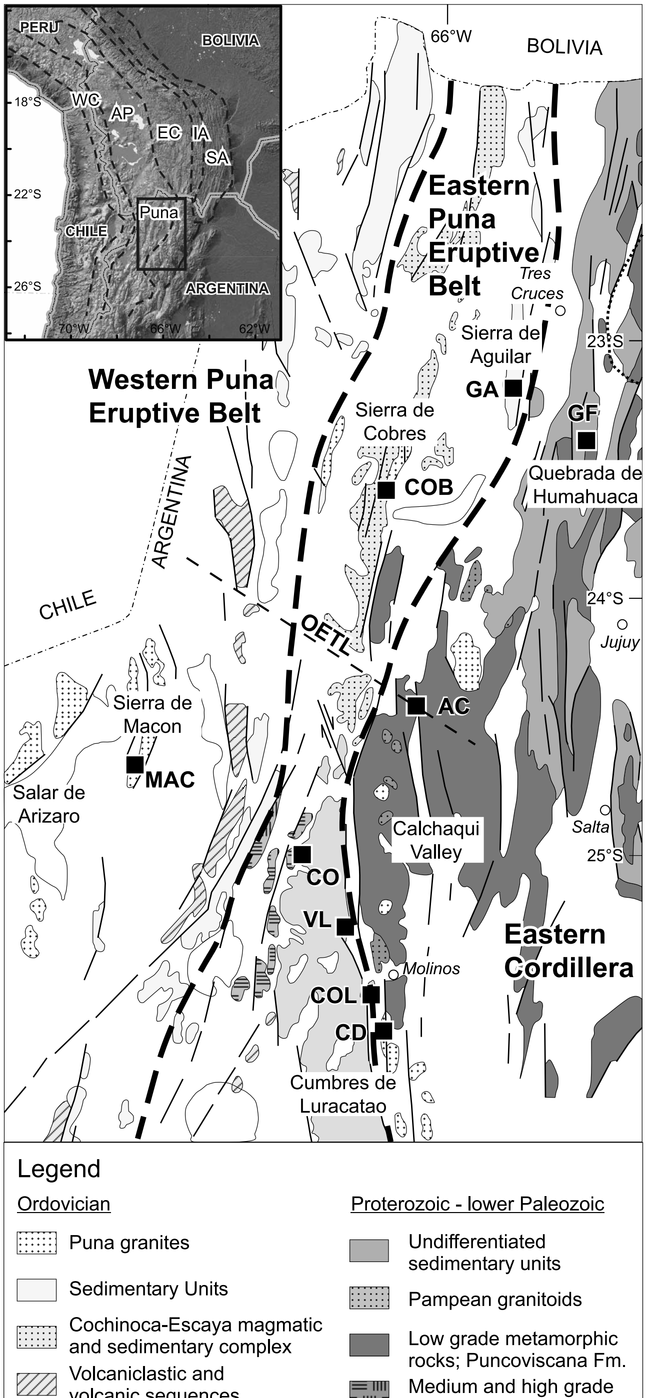

[3] What is known is that the present boundary between the Puna plateau and the Eastern Cordillera has a long history of regional tectonism and emplacement of granitoid magmas (Figure 1). Subduction along the Pacific coast of South America has triggered episodes of magmatism, basin formation, and tectonics in the central Andes since the early mid Ordovician (∼490–470 Ma) [*Coira et al.*, 1982]. Previous studies have mostly concentrated on detailed petrological-geochemical analyses of single plutons to understand their genesis [e.g., *Coira et al.*, 1999; *Poma et al.*, 2004; *Kirschbaum et al.*, 2006; *Hongn and Riller*, 2007] and established the geologic evolution of the central Andes during the early Paleozoic [e.g., *Coira et al.*, 1999]. The genesis, ascent and emplacement of Ordovician magmas along the present-day Puna and Eastern Cordillera boundary occurred in a complex back-arc setting that was associated with thermal anomalies and lithospheric thinning, and characterized by transpressional shortening episodes in an overall extensional regime [*Coira et al.*, 1999; *Kirschbaum et al.*, 2006; *Coira et al.*, 2009b]. Host rocks consisted of different tectonometamorphic domains with distinct metamorphic grades, rheologic properties [*Coira et al.*, 1982; *Coira et al.*, 1999], and linked ductile deformation zones that could have facilitated the ascent of magmas at deeper crustal levels [*Hongn and Mon*, 1999; *Hongn and Riller*, 2007].

[4] Recent studies of the Puna plateau, its eastern flanks, and the adjacent broken foreland suggest an irregular Cenozoic deformation pattern controlled by inherited crustal discontinuities [e.g., *Hongn et al.*, 2007]. Thus, the preexisting Paleozoic structural and stratigraphic heterogeneities may have influenced magmatism and subsequent deformation phases [e.g., *Mon and Hongn*, 1991; *Hongn and Riller*, 2007; *Carrera and Muñoz*, 2008; *Wegmann et al.*, 2008; *Hongn et al.*, 2010; *Pearson et al.*, 2012]. For example, the trend of Cretaceous intracratonic rift structures in northern Argentina is similar to the preexisting Paleozoic crustal anisotropies [e.g., *Galliski and Viramonte*, 1988; *Grier et al.*, 1991]. Moreover, many Mesozoic rift structures were reactivated and inverted during the Cenozoic Andean orogeny [*Grier et al.*, 1991; *Kley et al.*, 2005; *Mon et al.*, 2005]. In the Puna plateau region Mio-Pliocene volcanic

Figure 1. Geologic map of part of the Puna plateau margin in northwest Argentina showing the distribution of Ordovician and temporally related magmatic and sedimentary units (modified from *Rapela et al.* [1992] and *Coira et al.* [1999]). Map shows principle faults, salars (white areas) and cities (open circles). Generalized boundaries between the Western Puna Eruptive Belt, Eastern Puna Eruptive Belt, and Eastern Cordillera are shown as heavy dashed lines [after *Coira et al.*, 1999]. Black squares are sample locations of plutonic rocks (MAC = Sierra de Macón, CO = Complejo Oire, VL = Valle Luracatao, COL = Colomé, CD = Cerro Durazno, GA = Aguilar granite, GF = Fundiciones granite, COB = Cobres granite, AC = Nevado de Acay). OETL, Olacapato–El Toro lineament. Inset is a shaded 90 m SRTM DEM of the central Andes showing major morphological units (WC = Western Cordillera, AP = Altiplano, EC = Eastern Cordillera, IA = Interandean zone, SA = Subandes) [e.g., *Troëng et al.*, 1993; *Kley*, 1996] and location of study area (black box).

centers are concentrated along inherited NW oriented shear zones and magmas have exploited these zones of weakness to reach the surface [e.g., *Kay et al.*, 1994; *Riller and Oncken*, 2003].

[5] Unraveling the lower Paleozoic magmatism and thermal effects of successive tectonic phases throughout the Phanerozoic is key for understanding the geological and thermal history of the basement rocks that constitute the Puna plateau. In this study, we combine new U-Pb geochronology and $^{40}Ar/^{39}Ar$ thermochronology to constrain the Paleozoic and Mesozoic cooling histories of basement rocks along the eastern Puna/Eastern Cordillera boundary. We provide new age constraints on Paleozoic, Mesozoic and Tertiary plutons in the northern part of the Puna/Eastern Cordillera transition zone. By integrating our results with previously reported low-temperature apatite fission track (AFT) results [*Deeken et al.*, 2006] we (1) provide quantitative constraints on sample time-temperature histories from crystallization (∼850°C) to closure of the K-Ar system (∼350–150°C); (2) use our results to interpret differences in the amount of pre-Cenozoic denudation of the crust across different domains; and (3) explore the influence of inherited zones of crustal weakness on subsequent deformation phases. In particular, we present new age and uplift constraints for the Paleozoic, Mesozoic and early Cenozoic that influenced the locus of Cenozoic crustal deformation processes and the initial thermomechanical conditions for orogenic plateau growth.

2. Geological Setting

[6] The Altiplano-Puna plateau covers a region of ∼500,000 km^2 with an average elevation of ∼4 km across the central Andes [*Isacks*, 1988]. In this study, we focus on the structural transition from the eastern Puna margin to the Eastern Cordillera between 23°S and 26°S (Figure 1). At the present-day boundary between the Puna and the Eastern Cordillera, magmatic rocks comprise two NNW-SSE striking magmatic belts known as the Faja Eruptiva de la Puna Occidental in the west [*Palma et al.*, 1986] and Faja Eruptiva de la Puna Oriental in the east [*Méndez et al.*, 1973]. We refer to these two zones as the western and eastern Puna eruptive belts [e.g., *Coira et al.*, 2009b; *Coira et al.*, 2009a]. In addition, lower Paleozoic magmatic units are exposed farther east in the Eastern Cordillera (Figure 1). Most of the magmatism that characterizes the basement rocks of these geological provinces occurred in the lower to mid Ordovician ∼490–460 Ma [e.g., *Coira et al.*, 2009b, and references therein].

[7] Lower Paleozoic magmatic, sedimentary and metamorphic rocks are widely distributed throughout the study area. The western Puna eruptive belt includes granite-granodiorite-monzodiorite plutons that record three main magmatic episodes between 502 and 476 Ma, 450–440 Ma, and 420–425 Ma [*Mpodozis et al.*, 1983; *Palma et al.*, 1986; *Koukharsky et al.*, 2002; *Kleine et al.*, 2004]. The northern part of the eastern Puna eruptive belt is defined by greenschist-grade metasediments and the magmatic-sedimentary Cochinoca-Escaya Complex (Figure 1) [*Coira et al.*, 1999] with granitoids comprising ages of ∼480–470 Ma [*Lork and Bahlburg*, 1993; *Kirschbaum et al.*, 2006]. To the south, the Cochinoca-Escaya Complex is cut by undifferentiated higher-grade metamorphic assemblages [*Coira et al.*, 1982; *Damm et al.*, 1990]. Extensive magmatic units are exposed with ages of 500–462 Ma, 450–440 Ma, and 420 Ma [*Linares*, 1979; *Lork and Bahlburg*, 1993; *Lucassen et al.*, 2000]. Paleozoic pressure-temperature records suggest transient high temperatures (>650°C) and pervasive partial melting of the crust at ∼15–25 km depths at that time [*Lucassen and Franz*, 2005]. Farther east, Ordovician granitoids in the Eastern Cordillera mainly intruded into upper Precambrian to Cambrian turbiditic sequences of the Puncoviscana Formation [*Mon and Salfity*, 1995; *Coira et al.*, 1999]. Ordovician units were emplaced syntectonically and are characterized by linked NW-SE and N-S striking ductile shear zones and SW dipping metamorphic foliations [*Büttner et al.*, 2005; *Hongn and Riller*, 2007]. Deformation processes continue into the Silurian [*Turner and Méndez*, 1975; *Bahlburg*, 1990; *Wegmann et al.*, 2008] as part of mountain building processes at the western margin of Gondwana that included complex contraction and extension associated with left-lateral shearing [*Mon and Hongn*, 1991; *Bahlburg and Herve*, 1997; *Zimmermann and Bahlburg*, 2003; *Hongn and Riller*, 2007; *Coira et al.*, 2009b].

[8] Posttectonic Devonian-Carboniferous alkaline granitoids have been reported in the eruptive belts [*Rapela et al.*, 1992]. In the Carboniferous, anorogenic magmatism affected a large region of the present-day Argentine Sierras Pampeanas south of the study area [*Dahlquist et al.*, 2010]. Most of these granitoids were emplaced at high crustal levels along prominent older shear zones [*Höckenreiner et al.*, 2003; *Dahlquist et al.*, 2006] and intruded into host rocks of lower Paleozoic age [e.g., *Rapela et al.*, 1990; *Sims et al.*, 1998; *Pankhurst et al.*, 2000; *Grosse et al.*, 2009; *Dahlquist et al.*, 2010]. The generation of Carboniferous magmas is consistent with a regional reheating of the crust at ∼350–335 Ma [*Grissom et al.*, 1998; *Höckenreiner et al.*, 2003; *Dahlquist et al.*, 2006; *Alasino et al.*, 2012]. This period was followed by cooling and uplift in the late Carboniferous [*Höckenreiner et al.*, 2003; *Dahlquist et al.*, 2010]. Although Carboniferous magmatism is not evident in our study area, late Paleozoic transient heating of rocks in our study area associated with the anorogenic event is a possibility.

[9] An intracratonic rift system developed in northern Argentina during Cretaceous-Paleogene time (∼160–60 Ma) [*Salfity*, 1982; *Galliski and Viramonte*, 1988; *Salfity and Marquillas*, 1994; *Kley et al.*, 2005]. Rift-related igneous rocks are mainly hornblende-biotite granodiorites/granites that intrude early Cambrian (Puncoviscana Formation) or Ordovician sediments. The Salta rift was characterized by a series of NW to NE striking normal faults that bound horsts and grabens [e.g., *Galliski and Viramonte*, 1988; *Grier et al.*, 1991]. Many of the present-day faults that bound the igneous basement ranges investigated here are reactivated structures inherited from the Salta rift system [*Grier et al.*, 1991; *Mon et al.*, 2005]. Thus, Cretaceous plutons often occupy the hanging walls of thrust faults. Previous studies place the onset of rift inversion in the Puna region to Eo-Oligocene time (40–30 Ma) [*Andriessen and Reutter*, 1994; *Coutand et al.*, 2001; *Kley and Monaldi*, 2002], hence, prior to the superseding major phases of Andean deformation, uplift and exhumation that occurred during the Miocene in the eastern Puna [e.g., *Carrapa et al.*, 2005; *Coutand et al.*, 2006]. Deformation in the Puna remains active within the Plio-Quaternary [*Allmendinger et al.*, 1989; *Cladouhos et al.*, 1994; *Marrett et al.*, 1994; *Schoenbohm and*

Table 1. Sample Locations, U-Pb, and $^{40}Ar/^{39}Ar$ Analyses[a]

		Sample Characteristics			U-Pb Zircon			K-Feldspar $^{40}Ar/^{39}Ar$	
Sample	Location	Latitude (°S)	Longitude (°W)	Altitude (m)	Age ± 1σ SD (Ma)	MSWD[b]	Number of Grains	J Factor[c]	Total Gas Age ± 1σ SD (Ma)
MAC	Sierra de Macon[d]	24°35.687	67°19.585	4000	473.73 ± 4.33	0.96	7	0.003538	420.34 ± 6.20
CO	Complejo Oire[e]	25°00.345	66°41.941	3990	481.90 ± 4.19	0.80	5	0.003541	317.51 ± 4.63
VL	Valle Luracatao[e]	25°18.095	66°29.540	3150	491.20 ± 4.35	1.29	6	0.003539	237.69 ± 3.78
COL	Colome[e]	25°36.269	66°24.597	2570	468.80 ± 3.33	1.52	5	0.003544	293.02 ± 4.32
CD	Cerra Durazno[e]	25°39.292	66°20.971	2800	488.10 ± 3.12	0.78	7	0.003543	306.25 ± 4.48
COB	Cobres[e]	23°38.623	66°17.604	3800	478.40 ± 3.46	4.04	7	0.003549	172.28 ± 2.65
GF	Fundiciones granite[d]	23°23.526	65°26.813	3927	160.40 ± 1.20	0.68	7	0.003546	161.78 ± 2.66
GA	Aguilar granite[d]	23°12.856	65°41.217	4050	150.40 ± 0.91	2.77	7	0.003547	94.68 ± 1.55
AC	Nevado de Acay[e]	24°24.547	66°10.688	4986	12.61 ± 0.25	1.25	9	0.003545	15.17 ± 0.93

[a]Adjusted for atmospheric argon and nucleonic interferences $^{40}Ar/^{39}Ar_K$ = 0.0285; $^{36}Ar/^{37}Ar_{Ca}$ = 0.00018; $^{39}Ar/^{37}Ar_{Ca}$ = 0.00057.
[b]Mean square of weighted deviates.
[c]Irradiation factor.
[d]Corrected for ^{204}Pb.
[e]Corrected for $^{206}Pb/^{208}Pb$.

Strecker, 2009]. During the middle late Miocene, eruptions associated with stratovolcanoes along the modern magmatic arc were controlled by inherited Paleozoic northwest striking shear zones [*Coira et al.*, 1982; *Allmendinger et al.*, 1983; *Alonso et al.*, 1985; *Salfity*, 1985].

3. Methods

3.1. Sampling

[10] We sampled broadly to constrain the large-scale spatial variations in basement thermal histories. We targeted well-exposed early Paleozoic plutonic rocks and overlying strata along the eastern Puna/Eastern Cordillera boundary region because they are potentially capable of preserving pre-Andean cooling signals (Table 1 and Figure 1). In general, samples were located close to the base of mountain ranges at 2.5–5.0 km elevations. We analyzed Ordovician basement rocks from the western Puna eruptive belt (Sierra de Macón = MAC), the eastern Puna eruptive belt (Cobres granite = COB, Complejo Oire = CO, Valle Luracatao = VL, Colomé = COL), and the Eastern Cordillera (Cerro Durazno = CD). We also analyzed two Cretaceous samples from the northern Puna/Eastern Cordillera boundary (Aguilar granite = GA, Fundiciones granite = GF), and one Tertiary sample along a NW-SE trending crustal lineament (OETL in Figure 1) in the Eastern Cordillera (Nevado de Acay = AC). For each sample, we collected ∼3 kg of rock and isolated zircon and K-feldspar crystals using standard crushing, sieving, and density/magnetic separation techniques. We then used a binocular microscope to hand-select specific grains for our analysis.

3.2. Zircon U-Pb Geochronology

[11] The U-Pb isotope system is used to infer crystallization ages of magmatic zircon. Results of U-Pb ion microprobe analysis of 63 zircons from 9 granite samples (5–7 zircons per sample) are summarized in Figure 2 and Table 1. Complete methods and tabulated data are presented in the auxiliary material.[1] Cathodoluminescence (CL) imaging generally revealed that core-rim overgrowth textures were uncommon. However, we did observe more complex textural relationships on a few individual grains (e.g., VL grain 6; Figure 2c). Our analysis spots were deliberately placed near the grain margins in order to probe the youngest growth layers and to avoid the older zircon interiors. Thus, while older (Grenville) ages documented for the Sierras Pampeanas [e.g., *Casquet et al.*, 2005] were not detected in our analyses, no firm conclusion regarding inheritance of this age should be drawn since we did not measure grain interiors.

3.3. K-Feldspar $^{40}Ar/^{39}Ar$ Thermochronology

[12] K-feldspar $^{40}Ar/^{39}Ar$ thermochronology provides the basis for reconstructing the thermal history of the Andean crust [e.g., *McDougall and Harrison*, 1999]. Determination of thermal histories from $^{40}Ar/^{39}Ar$ step heating of K-feldspars is based upon MultiDiffusion Domain (MDD) analysis [e.g., *McDougall and Harrison*, 1999]. In favorable circumstances, MDD modeling has proven capable of yielding continuous thermal histories between 350°C and 150°C [*Lovera et al.*, 1989, 1997, 2002; *Harrison et al.*, 2005]. Application of MDD modeling to $^{40}Ar/^{39}Ar$ results from K-feldspar requires assumptions about the general form of the temperature-time path taken by any sample. We restrict our interpretation to the simplest possible solution, i.e., monotonic cooling.

[13] Assuming monotonic cooling, calculated thermal histories obtained from $^{40}Ar/^{39}Ar$ K-feldspar step heating typically define a narrow range of possible temperature–time conditions [*Lovera et al.*, 1997]. MDD modeling approaches have been developed that provide useful constraints on potential nonmonotonic cooling paths such as maximum bounds on peak temperatures associated with reheating [*Quidelleur et al.*, 1997; *McDougall and Harrison*, 1999; *Harrison et al.*, 2000; *Lovera et al.*, 2002]. However, MDD-derived models cannot unambiguously distinguish monotonic from nonmonotonic cooling paths without additional information. With the lack of independent thermal history constraints in our study area, removing the monotonic assumption would significantly increase the range of potential model thermal histories, preclude the straightforward use of closure temperature concepts, and introduce

[1]Auxiliary material data sets are available at ftp://ftp.agu.org/apend/tec/2012tc003168. Other auxiliary material files are in the HTML. doi:10.1029/2012TC003168.

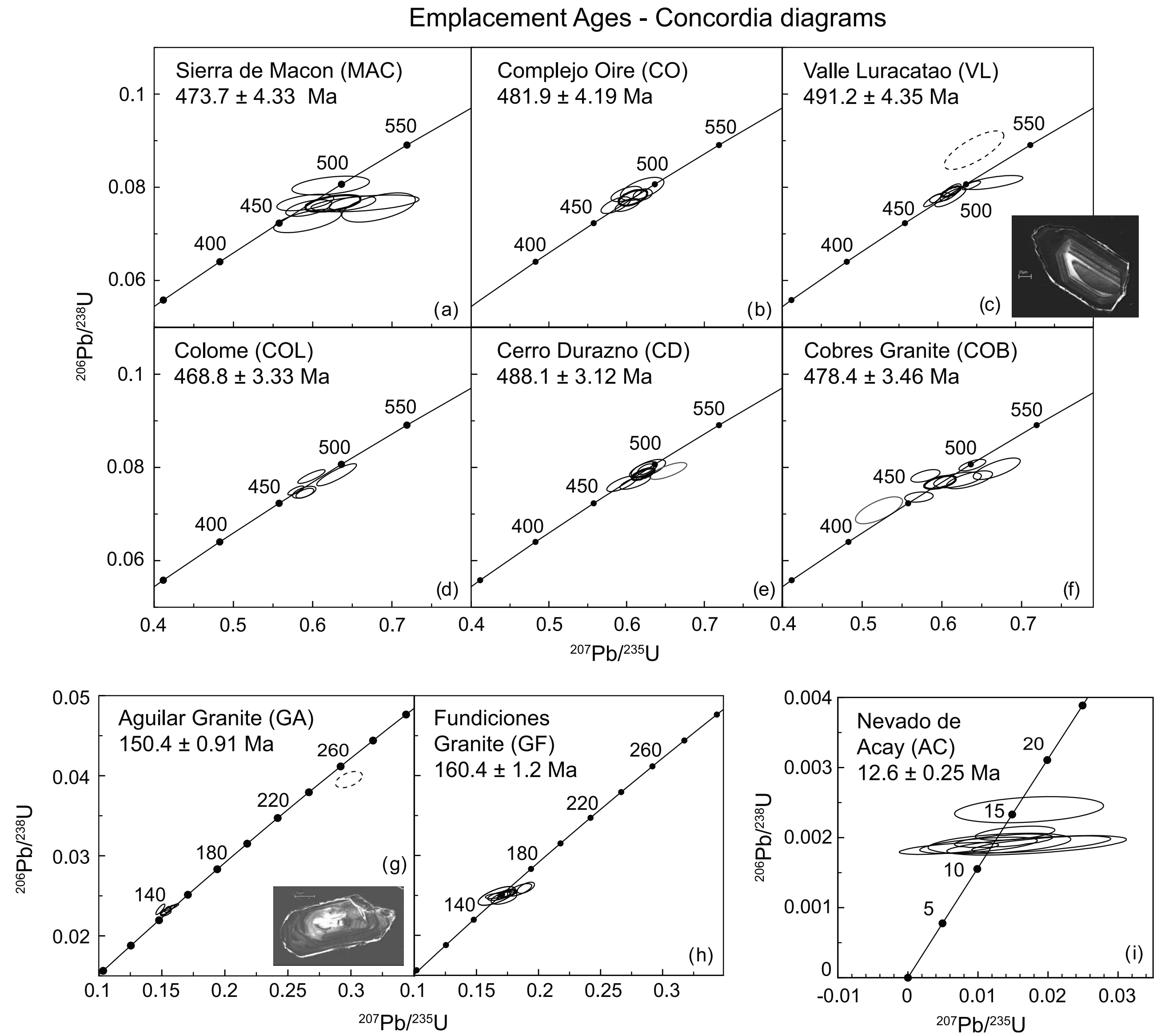

Figure 2. The ^{206}U/^{238}U versus ^{207}U/^{235}U Concordia diagrams for U-Pb ion microprobe results for zircons from nine different samples. The individual analysis results are plotted as open (1 sigma errors) ellipses, bold ellipses are error ellipses, dashed ellipses represent analyses excluded from calculating the mean age. CL images show grain VL_g6 (Figure 3c) and GA_g6 (Figure 3g).

ambiguities in modeling continuous time–temperature paths [*Reiners*, 2009]. Because we have no clear indication of transient heating by nearby plutons or any other sources of crustal heat addition between early Silurian and Cretaceous times, we adopt the assumption of monotonic cooling as the most sensible first-order interpretation of the feldspar ^{40}Ar/^{39}Ar data.

[14] Some K-feldspars have been shown to yield anomalously old ^{40}Ar/^{39}Ar ratios over the first several percent of ^{39}Ar release, which has been attributed to thermal decrepitation of excess argon (^{40}Ar$_E$) bearing fluid inclusions [*Harrison et al.*, 1994]. To improve the basis for correcting the low-temperature argon release from these feldspars, we performed isothermal quadruplicates with the low-temperature steps. Since the number of fluid inclusions that burst at a given temperature decreases with progressive heating, the first isothermal step is interpreted to yield an anomalously old age, while the second and successive steps are less affected, and thus yield younger ages. Generally, ^{40}Ar$_E$ is correlated with Cl/K and an age spectrum correction for the effects of low-temperature ^{40}Ar$_E$ contamination is possible [*Harrison et al.*, 1993, 1994]. However, corrections for Cl-correlated ^{40}Ar$_E$ were ineffective for our samples due to a combination of high ^{40}Ar$_E$/Cl and low Cl/K values that resulted in erratic corrected ages because they were overly sensitive to measurement uncertainties in Cl/K (i.e., only a small % of measured ^{38}Ar was Cl derived). Thus, to avoid interpretative difficulties in modeling the age spectrum, we did not attempt to fit the lowest-temperature portion of the age spectrum that is characteristically degraded by fluid inclusion-hosted ^{40}Ar$_E$.

[15] Another feature often manifested by samples are low-amplitude intermediate age maxima in the age spectra. Such features may result from recrystallization of diffusion domains after the onset of ^{40}Ar retention [*Lovera et al.*, 2002]. Suspected physical phenomena include low-temperature exsolution or partial alteration to albite and other phases and/or new growth of low-temperature adularia [e.g., *Parsons et al.*, 1999; *Lovera et al.*, 2002]. The impact of these phenomena is that newly formed, small domains inherit the ^{40}Ar concentrations from their larger precursor domains [see *Lovera et al.*, 2002]. Consequently, thermal history results from affected samples are generally less reliable than those for samples lacking such features. However, in cases where prominent intermediate age maxima occur for our samples (e.g., Sierra de Macón), the uncertainties associated with detailed MDD thermal history analysis is minimized because samples cooled rapidly.

[16] Table 1 summarizes the key ^{40}Ar/^{39}Ar results with correction factors for interfering neutron reactions determined from CaF_2 and K_2SO_4 crystals and calculated J factors. Detailed analytical results for individual analyses are provided in the auxiliary material. For each sample, we calculated 10 best fit MDD parameter sets. Five best fit monotonically decreasing cooling histories were calculated from each set of MDD parameters to yield 50 total solutions. Using these solutions, we determined the 90% confidence limits of the thermal history that correspond to the interpreted portion of the age spectrum.

4. Results

4.1. Zircon U-Pb Data and Analysis

[17] Most of the 63 zircon grain analyses have concordant ^{206}Pb/^{238}U ages (Figure 2). After excluding anomalous age results (e.g., grain 6 for GA and VL, Supp2), weighted mean ^{206}Pb/^{238}U ages were calculated for the remaining analyses. Generally, values of the mean square of weighted deviates (MSWD) fell within the expected range for a homogenous population [*Mahon*, 1996]. With these samples, we interpret the results to characterize the age of magmatic crystallization within 1σ analytical uncertainties. The two exceptions are samples from the Cobres granite and the Aguilar granite with MSWD values of 4.0 and 2.8, respectively. While the age spread may signal heterogeneity in the zircon population (e.g., caused by inheritance or Pb loss), we adopted a conservative approach of increasing the stated uncertainties on the sample mean age by the square root of the MSWD.

4.1.1. Ordovician Granitoids

[18] The Sierra de Macón is an elongated basement range within the Puna (Figure 1). It is the easternmost granitoid of the Ordovician western Puna belt [*Poma et al.*, 2004]. Our ^{206}Pb/^{238}U data indicate a crystallization age of 473.7 $\pm$ 4.3 Ma (Table 1 and Figure 2a). This age is consistent with radiometric ages determined by previous workers (^{40}Ar/^{39}Ar on hornblende: 482.7 $\pm$ 7.8 Ma [*Koukharsky et al.*, 2002]) and agrees with regional age relationships for early Ordovician intrusions [e.g., *Coira et al.*, 1999].

[19] Four samples were obtained from the southern transition between the eastern Puna and the Eastern Cordillera (Figure 1). Our Ordovician samples mostly consist of biotite-hornblende bearing granodiorite and monzogranite and K-feldspar-rich granites thrust over Tertiary red beds. The Complejo Oire sample is from the western border of the fault–bounded Cumbres de Luracatao range, whereas the Valle de Luracatao and Colomé samples are from the eastern flank that forms the western margin of the Luracatao valley (Figure 1). Our southernmost sample is from the Cerro Durazno range, which is part of a series of $\sim$30 km long en échelon structural blocks that border the southeastern Puna plateau [*Allmendinger*, 1986]. Samples yielded weighted mean ^{206}Pb/^{238}U ages between 469 and 491 Ma (481.9 $\pm$ 4.2 Ma (Complejo Oire), 491.2 $\pm$ 2.8 Ma (Valle Luracatao), 468.8 $\pm$ 3.3 Ma (Colomé), 488.1 $\pm$ 3.1 Ma (Cerro Durazno); Table 1 and Figures 2b–2e). We also sampled the Cobres pluton along the northeastern Puna margin (Figure 1). The zircons have a weighted mean ^{206}Pb/^{238}U age of 478.4 $\pm$ 3.5 Ma (Table 1 and Figure 2f). All of these ages fall into the early to middle Ordovician and correlate with reported ages from the eastern Puna belt [e.g., *Omarini et al.*, 1984; *Lork and Bahlburg*, 1993; *Coira et al.*, 1999; *Viramonte et al.*, 2007; *Pearson et al.*, 2012].

4.1.2. Cretaceous Granitoids

[20] Our Cretaceous samples are located at the northern margin of our study area between the eastern Puna and the Eastern Cordillera and include the Aguilar granodiorite and the Fundiciones granite (Figure 1). Zircon U-Pb weighted mean ages are 150.4 $\pm$ 0.9 Ma for the Aguilar granodiorite and 160.4 $\pm$ 1.2 Ma for the Fundiciones granite (Table 1 and Figures 2g and 2h). The Aguilar age is significantly older than previously determined Rb/Sr crystallization ages and K-Ar ages of 110–133 Ma [*Halpern and Latorre*, 1973]. Although one zircon (g6) was clearly inherited ($\sim$250 Ma), CL imaging of the grains showed that the ion microprobe analysis sites successfully avoided inherited zircon domains, and hence support a late Jurassic crystallization age. This age is consistent with ^{206}Pb/^{238}U ages of the Abra Laite pluton just west of the Aguilar that has an average age of $\sim$153 Ma as well as the 140–153 Ma old Tusaquillas Plutonic Complexes $\sim$35 km to the south [*Cristiani et al.*, 2005].

4.1.3. Tertiary Plutons

[21] The Nevado de Acay pluton is the youngest intrusion we sampled. This biotite- and hornblende-bearing quartz-monzonite intruded low-grade metamorphic rocks of the Puncoviscana Formation and Upper Cretaceous limestones and pelites of the Yacoraite Formation in the Calchaqui Valley (Figure 1). The location of the pluton is thought to have been structurally controlled by the Olacapato–El Toro lineament (OETL) [*Llambias et al.*, 1985]. Eight zircons yielded concordant ^{206}Pb/^{238}U results with a weighted mean age of 12.6 $\pm$ 0.3 Ma (Table 1 and Figure 2i). Although previous ages indicated late Oligocene (26 $\pm$ 1 Ma [*Mirre*, 1974; *Linares*, 1979]) or early Miocene emplacement (18–19 Ma [*Petrinovic et al.*, 1999]), our new younger age is more compatible with similar magmatic rocks in the region [*Petrinovic et al.*, 1999; *Mazzuoli et al.*, 2008; *Kay et al.*, 2010].

4.2. K-Feldspar ^{40}Ar/^{39}Ar Thermal Histories

[22] In the following, we describe sample cooling histories organized by their locations within the broad tectonic framework (western Puna eruptive belt, southeastern Puna/Eastern Cordillera boundary, northeastern Puna/Eastern Cordillera transition). Deriving depth estimates is difficult

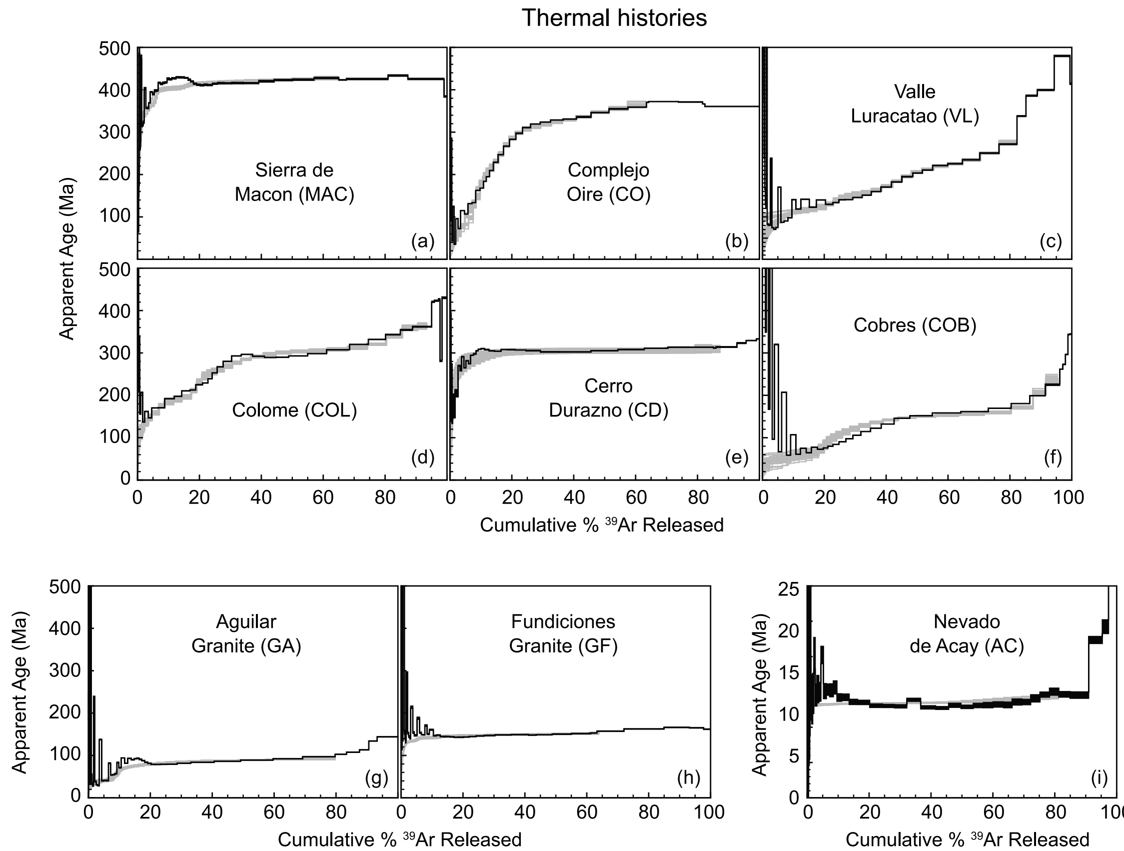

Figure 3. Thermal history results constrained by the K-feldspar $^{40}Ar/^{39}Ar$ data. The measured age spectrum and model fits produced by best fit thermal histories; gray line indicates MDD model fit, black line indicates laboratory values. Dashed lines are inferred histories between the regions constrained by the data.

due to uncertainties in the paleogeothermal gradient. Modern temperature gradients in boreholes in the central Andes are 39 ± 9°C/km in the plateau area and 25 ± 8°C/km in the Eastern Cordillera [*Henry and Pollack*, 1988; *Springer and Förster*, 1998]. Estimated Cenozoic paleogeotherms in the central Andes range between 32 and 19°C/km with errors of 20–40% [e.g., *Carrapa et al.*, 2006; *Deeken et al.*, 2006; *Ege et al.*, 2007]. Thus, we estimate depths assuming an average paleogeothermal gradient of 25–35°C/km, applying the higher geotherm to most of the Paleozoic and Mesozoic estimates and the lower geotherm to Cenozoic times. These geotherms represent temperatures for an equilibrated crust and cannot be applied to intrusions. Thus, estimated crystallization depths are based on (1) the overall cooling history (i.e., how fast the sample cools down after crystallization) and (2) previously estimated crystallization pressures and temperatures in the central Andes (i.e., assuming generally shallow intrusion depths at pressure <0.4 GPa and/or 4–8 km [*Kay et al.*, 2010, and references therein]).

4.2.1. The Western Puna Eruptive Belt

[23] K-feldspar $^{40}Ar/^{39}Ar$ step heating of the Sierra de Macón sample shows a minor age gradient between 410 and 430 Ma over the last 80% of ^{39}Ar release (Figure 3a). The initial gas released exhibits an age gradient down to 250 Ma before it is obscured by initial low-temperature $^{40}Ar_E$ contamination. Although the detailed temperature-time history is slightly uncertain due to the prominent intermediate age maxima at ~10% ^{39}Ar release, our calculations indicate that it does not seriously impact our ability to extract the MDD thermal history, because the sample cooled rapidly.

[24] MDD modeling results indicate temperatures <300°C by ~420 Ma (Figure 4a and Table 2), suggesting shallow crystallization depths (<8 km?). Importantly, the Sierra de Macón cooled very rapidly (~3.6°C/Myr) to ~150°C by ~370 Ma, followed by a long period of thermal crustal stability with slow cooling (<0.2°C/Myr). The Sierra de Macón stayed at 150–120°C (~4 km depth) throughout most of the late Paleozoic and early Mesozoic. AFT data indicate cooling below ~115°C at ~200 Ma [*Deeken et al.*, 2006].

4.2.2. The Southeastern Puna/Eastern Cordillera Boundary

[25] K-feldspar $^{40}Ar/^{39}Ar$ data from samples along the eastern Puna eruptive belt indicate a monotonically increasing age spectrum (Figures 3b–3d and 3f). The southern Puna samples indicate cooling to <300°C between 400 and 360 Ma (Figures 4b–4d and Table 2). Temperatures remained above 200°C (>6–8 km depth) until Jurassic/Cretaceous time. The Complejo Oire and Valle de Luracatao granites cooled slowly (~0.2–0.3°C/Myr) during the Paleozoic and the early Mesozoic. Both samples experienced rapid cooling in the late Jurassic/early Cretaceous with cooling rates increasing from <0.2 to 0.6°C/Myr (Complejo Oire) and 0.3 to 1.3°C/Myr (Valle Luracatao), respectively (Figures 4b and 4c and Table 2). The Colomé sample is

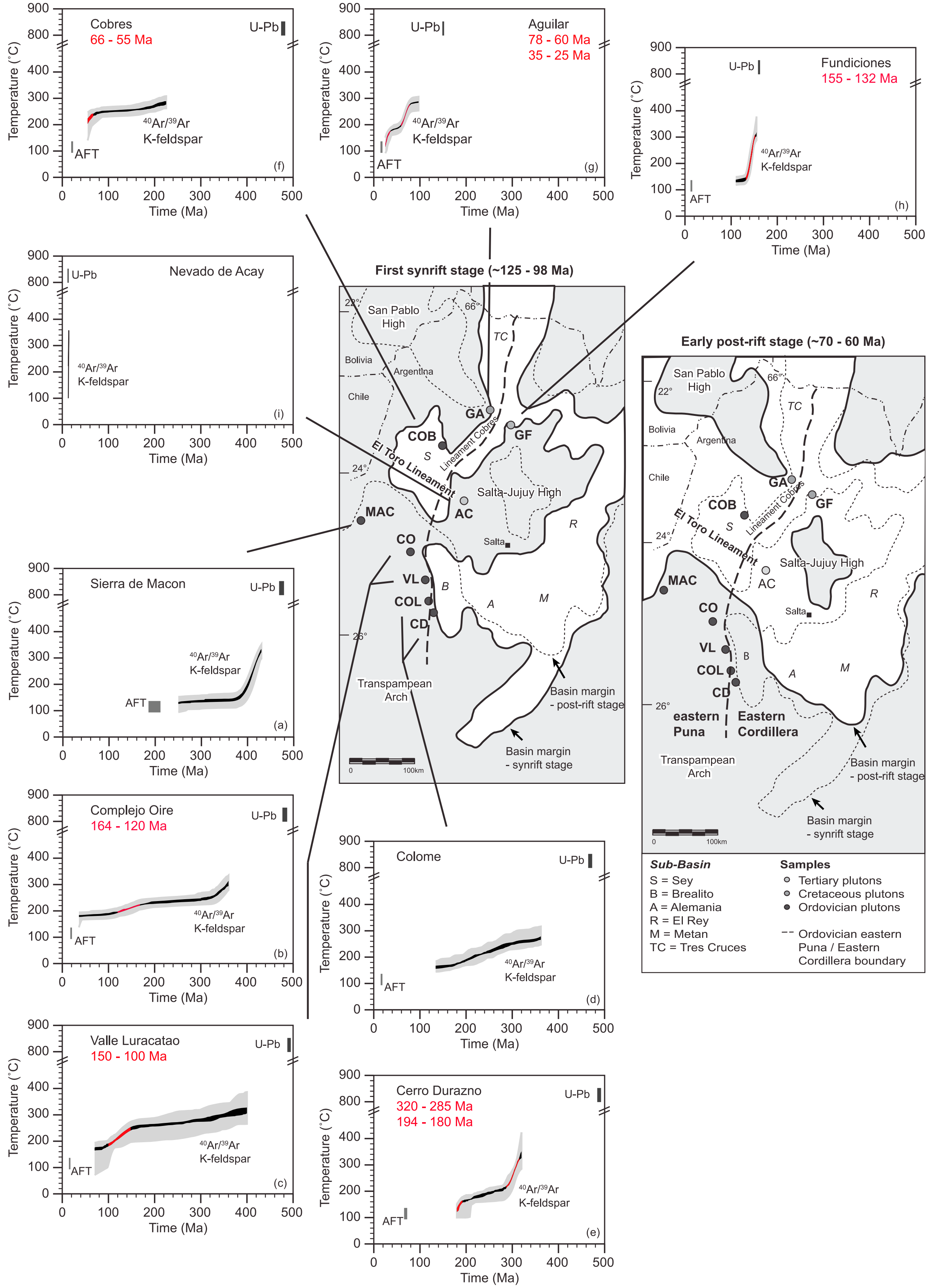
Cobres
66 - 55 Ma
Aguilar
78 - 60 Ma
35 - 25 Ma
Fundiciones
155 - 132 Ma
Nevado de Acay
Sierra de Macon
Complejo Oire
164 - 120 Ma
Valle Luracatao
150 - 100 Ma
Colome
Cerro Durazno
320 - 285 Ma
194 - 180 Ma
U-Pb
AFT
40Ar/39Ar
K-feldspar
Temperature (°C)
Time (Ma)
First synrift stage (~125 - 98 Ma)
Early post-rift stage (~70 - 60 Ma)
San Pablo High
Bolivia
Argentina
Chile
TC
GA
GF
COB
S
Lineament Cobres
El Toro Lineament
Salta-Jujuy High
AC
MAC
CO
VL
COL
CD
B
A
M
R
Salta
Transpampean Arch
Basin margin - post-rift stage
Basin margin - synrift stage
eastern Puna
Eastern Cordillera
Sub-Basin
S = Sey
B = Brealito
A = Alemania
R = El Rey
M = Metan
TC = Tres Cruces
Samples
Tertiary plutons
Cretaceous plutons
Ordovician plutons
Ordovician eastern Puna / Eastern Cordillera boundary

Figure 4

Table 2. Cooling History[a]

Sample	Location	Time (Ma)	Temperature (°C)	Cooling Rate (°C/Myr)
		Sample Characteristics		
MAC	Sierra de Macon	430–380	330–150	3.60
		380–250	150–130	<0.2
		198.40	115	0.30
CO	Complejo Oire	360–320	304–250	1.35
		320–164	250–220	<0.2
		164–120	220–195	**0.57**
		120–36	195–180	<0.2
		19.10	115	**3.80**
VL	Valle Luracatao	400–150	315–248	0.27
		150–100	248–185	**1.26**
		100–70	185–170	0.50
		15.60	115	**1.00**
COL	Colome	362–134	275–160	0.50
		16.90	115	0.38
CD	Cerra Durazno	**320–283**	338–211	**3.43**
		283–194	211–162	0.55
		194–180	162–128	**2.43**
		69.40	115	0.29
COB	Cobres	225–66	283–235	0.30
		66–55	235–213	**2.00**
		21.30	115	**2.91**
GF	Fundiciones granite	**155–132**	312–142	**7.39**
		132–110	142–133	0.41
		13.9	115	<0.2
GA	Aguilar granite	97–78	285–275	0.53
		78–60	275–200	**4.17**
		60–35	200–173	1.08
		35–25	173–120	**5.30**
		16.70	115	0.60

[a]Bold values indicate accelerated cooling phases.

characterized by slow cooling to temperatures of ~160°C (~4.5–6 km depth) by 134 Ma (Figure 4d).

[26] The Cerro Durazno range is proximal to the present-day southern Puna margin, but located within the Eastern Cordillera. The K-feldspar $^{40}Ar/^{39}Ar$ step heating data show a flat age spectrum at ~320 Ma (Figure 3e). Detailed interpretation of the Cerro Durazno results is complicated by a minor intermediate age maximum at ~10% ^{39}Ar released, and the sample's low apparent activation energy [*Lovera et al.*, 1997]. However, MDD modeling results indicate that temperatures <300°C are not reached until ~300 Ma (i.e., much later than in the eastern Puna), while low temperatures of ~130°C are evident by 180 Ma (i.e., much earlier than for the eastern Puna samples; Figure 4e and Table 2). Two short phases of rapid cooling occur between 320–285 Ma (3.4°C/Myr) and 195–180 Ma (2.4°C/Myr) separated by slower cooling throughout the Permian and Triassic (Figure 4e). The shallow Cretaceous crustal depth (~4–5 km) implied by the Jurassic MDD results is consistent with an old AFT age of 69 ± 2 Ma [*Deeken et al.*, 2006], indicating a temperature below ~115°C since the latest Cretaceous.

4.2.3. The Northern Eastern Puna/Eastern Cordillera Transition

[27] The Cobres granite K-feldspar $^{40}Ar/^{39}Ar$ data have a monotonically increasing age spectrum (Figure 3f). This sample cooled to <300°C by ~230 Ma (Figure 4h). Although its thermal history is poorly constrained below ~210°C, slow cooling (0.3°C/Myr) is evident throughout the Mesozoic. Cooling rates start to increase to ~2°C/Myr in the early Tertiary (Figure 4h and Table 2).

[28] K-feldspar $^{40}Ar/^{39}Ar$ results indicate a late Jurassic crystallization age for the Aguilar pluton. Specifically, the high-temperature release steps yield $^{40}Ar/^{39}Ar$ ages that closely approach the ~150 Ma crystallization age (Figure 3g). A minor intermediate age maximum between 10 and 20% ^{39}Ar released hampers our ability to calculate a thermal history from these results. Nevertheless, the results indicate a protracted residence above 300°C (>8.5 km depth) prior to 100 Ma (Figure 4g). The Aguilar intrusion is reported to be fault controlled [*Cristiani et al.*, 2005], but low temperatures of <120°C (<4–5 km depth) are not attained before 25 Ma. The Aguilar granite records two periods of rapid cooling (~4–5°C/Myr) during the late Cretaceous-Paleocene (78–60 Ma) and the Oligocene (34–25 Ma) with slower cooling (~1°C/Myr) during the intervening Eocene interval (Figure 4g). Although Miocene AFT data from this sample (16.6 ± 1.2 Ma [*Deeken et al.*, 2005]) are not inconsistent with our cooling history, thermal AFT modeling utilizing track length distributions could not simultaneously fit both the K-feldspar MDD and apatite thermal history constraints (A. Deeken, personal communication, 2012). One reason for the discrepancy could be the low number of datable grains and the scarcity of confined tracks in the AFT data (A. Deeken, personal communication, 2012).

[29] In contrast, the Fundiciones granite does not show protracted slow cooling above 300°C during the Cretaceous and instead has a flat age spectrum at ~150 Ma (Figure 3h). Rapid cooling (~7.4°C/Myr) occurred shortly after initial crystallization during the late Jurassic and early Cretaceous. This sample cooled to temperatures of ~150°C by 130 Ma (Figure 4g and Table 2). Subsequent cooling is characterized by an abrupt decrease in cooling rate to ~0.2–0.4°C/Myr without further rapid cooling. An AFT age of ~13.9 ± 0.9 Ma implies that the sample continued to reside at ~4–5 km depth until the middle Miocene [*Deeken et al.*, 2005].

4.2.4. Eastern Cordillera Tertiary Plutons

[30] The Ar age spectrum for the Nevado de Acay has a well-defined plateau at ~12 Ma (Figure 3i). We attribute the age discrepancy between $^{206}Pb/^{238}U$ zircon and $^{40}Ar/^{39}Ar$ K-feldspar to minor $^{40}Ar_E$ contamination of the K-feldspar and note that similar problems may have influenced earlier K-Ar studies [*Mirre*, 1974; *Linares*, 1979]. Regardless, rapid

Figure 4. Thermal histories from MDD modeling of K-feldspar $^{40}Ar/^{39}Ar$ age spectra. Dark and light shadings represent 90% confidence intervals for the mean values and overall distributions, respectively. Red segments indicate accelerated cooling phases discussed in the text. Also shown are apatite fission track (AFT) ages from *Deeken et al.* [2005]. Maps show the late Jurassic to late Cretaceous evolution of the Salta rift from synrift to early postrift stage with the horst (gray areas) and graben (white areas) structures (modified from *Marquillas et al.* [2005]). Note the cooling history differences for samples in the Eastern Cordillera and along the northern Puna margin; the southern plutons indicate faster cooling during the synrift stage, whereas the northern plutons indicate faster postrift-related cooling rates.

cooling after pluton emplacement is consistent with both shallow emplacement and rapid exhumation (Figure 4i).

4.3. Summary

[31] The $^{40}Ar/^{39}Ar$ K-feldspar analyses indicate diverse Paleozoic to early Cenozoic cooling histories in the Puna/Eastern Cordillera transition zone. The western Puna (Sierra de Macón sample) indicates stable and relatively cool crustal conditions characterized by slow cooling from below ~200°C (<6–8 km depth) since 400 Ma. Samples from the southeastern Puna were hotter overall and experienced slow cooling between 300°C and 200°C between the Devonian and Cretaceous with temperatures of ~200°C (~6–8 km depth) attained by 120 Ma. These samples (Complejo Oire, Valle de Luracatao, Colomé) reflect crustal thermal stability during most of Paleozoic and early to mid-Mesozoic times, followed by increased cooling rates during the early Cretaceous (~160–100 Ma). In contrast, the Cerro Durazno in the southern Eastern Cordillera cooled below 200°C by early Permian time (~270 Ma) and indicates rapid cooling in the early and middle Jurassic (~194–180 Ma).

[32] The northern Puna (Cobres and Aguilar granites samples) experienced slow protracted cooling until the late Cretaceous and faster cooling rates during the late Cretaceous/early Paleocene (78–55 Ma). Temperatures of <200°C (<6–8 km depth) were not attained until the Paleocene (60–55 Ma). These samples also show accelerated cooling during the Eocene. The northern Eastern Cordillera (Fundiciones granite) indicates rapid cooling in the early Cretaceous, reaching temperatures of <200°C by ~140 Ma, almost immediately following pluton emplacement. There is no independent evidence that the Fundiciones and Aguilar plutons initially crystallized at different depths. However, the initial rapid cooling of the Fundiciones from crystallization temperatures to ~150°C within 30 Ma and subsequent residence of the pluton between 150°C and 115°C strongly suggests either very shallow intrusion depths and/or very rapid magma ascent along faults. In contrast and despite its close proximity to rift bounding faults, the Aguilar granite resided at higher temperature throughout the Cretaceous and Paleogene, suggesting somewhat deeper intrusion levels.

5. Discussion

[33] Our new geochronologic data set provides insights into the exhumation history of pre-Cretaceous igneous basement rocks underlying the Puna and Eastern Cordillera in northwestern Argentina. The Eastern Cordillera and Puna regions have previously been characterized as having distinct pre-Paleozoic metamorphic and magmatic histories [e.g., *Ramos*, 2008]. Our data emphasize that these domains exhibit substantial contrasts in their Paleozoic and Mesozoic cooling histories. Furthermore, differences also exist between rock samples analyzed from within the northeastern and southeastern Puna/Eastern Cordillera transition. In sections 5.1–5.3, we discuss these differences in the context of the regional Paleozoic, Mesozoic, and Cenozoic tectonic history and compare them to existing thermal history information.

5.1. Paleozoic Evolution

[34] Evidence from high-grade rocks of northern Chile and northwestern Argentina implies high-temperature, low-pressure conditions of metamorphism, and a high thermal gradient at midcrustal levels during the early Paleozoic [*Lucassen et al.*, 1996]. Previous K-Ar analyses indicate cooling of metamorphic rocks in the western Puna belt to temperatures of ~500°C at ~480–450 Ma [*Lucassen et al.*, 1996] and ~300°C at 400 Ma [*Lucassen et al.*, 2000; *Damm et al.*, 1990; *Maksaev*, 1990]. Thus, initial rapid cooling of the Sierra de Macón below 300°C prior to the Devonian, and subsequent cooling to ~150°C by the earliest Jurassic (Figure 4a), points to protracted crustal residence at shallow depths (~8–4 km?) during this interval, assuming a geothermal gradient of 35°C/km. Protracted upper crustal residence is consistent with suggested fast subsidence rates in an early Ordovician back-arc basin in that region [*Mon and Salfity*, 1995; *Coira et al.*, 1999] and suggests the establishment and persistence of a relatively stable thermal regime following earlier Ordovician tectonism and magmatism [e.g., *Bahlburg and Herve*, 1997]. Patterns of subsidence and facies distribution are compatible with the emplacement of supracrustal loads of 8 km thickness on the western margin of the Puna basin [*Bahlburg and Furlong*, 1996]. Inverse thermal modeling of AFT data from the Arizaro basin just west of the Sierra de Macón [*Carrapa et al.*, 2009] indicates shallow crustal levels of ~140°C (~4 km) were achieved by ~200 Ma.

[35] Emplacement of Ordovician plutons in the region of the present-day eastern Puna and the Eastern Cordillera was coeval with regional deformation under high-temperature metamorphism [*Becchio et al.*, 1999; *Hongn and Riller*, 2007; *Wegmann et al.*, 2008]. Similar ages for all granitoids signifies simultaneous thermal events within the crust across the study area with abundant magmatism and intrusion at middle to lower crustal levels [*Lucassen et al.*, 2002]. This scenario has been either associated with Famatinian continental arc magmatism [e.g., *Coira et al.*, 2009b; *Otamendi et al.*, 2010] or a broad "mobile" belt of thickened crust and magmatic activity [*Lucassen et al.*, 2000]. Crustal temperatures of ~400–300°C by ~416–400 Ma have been reported in the Sierra de Quilmes, ~50 km to the south [*Büttner et al.*, 2005]. Our Luracatao range samples (Complejo Oire, Valle de Luracatao, Colomé) show protracted cooling throughout the Paleozoic with temperatures <300°C reached by the Devonian. A mechanically stable and shallow crust at this time is supported by a general lack of a post-Ordovician sedimentary record in northwestern Argentina prior to the latest Carboniferous [*Bahlburg and Herve*, 1997] and little to no metamorphism in the Cochinoca-Escaya complex sedimentary units [*Bahlburg*, 1990; *Coira et al.*, 1999].

[36] In contrast, the Cerro Durazno granite in the southern Eastern Cordillera and the Cobres granite in the northern Puna indicate significant differences in their cooling histories, implying regional variations in the thermal and structural regimes. Relative to the other samples, the Cerro Durazno and Cobres granites resided at higher temperatures (>300°C) until the late Paleozoic. These higher temperatures could imply either somewhat deeper crustal levels (>8 km) or unrecognized transient heating. A somewhat deeper crystallization depth at midcrustal levels is consistent with observations indicating that the emplacement of the Cerro Durazno and Cobres plutons was coeval with regional deformation under high-temperature metamorphism [*Hongn*

and Riller, 2007]. Furthermore, emplacement of these granitoids has been genetically related to prominent shear zones [*Hongn et al.*, 1999; *Hongn and Riller*, 2007; *Wegmann et al.*, 2008]. The proximity between brittle or ductile deformation zones and magma ascent and emplacement suggests that tectonically assisted transport and emplacement of magma occurred [*Hongn and Riller*, 2007]. Thus, despite significantly less erosion levels north of the OETL, a deeper crustal residence of the Cobres granite is reasonable, assuming that nearby faults assisted in subsequent exhumation of the granitoid. Deformation and plutonism is known to have occurred in the early Carboniferous, followed by the development of intracratonic basins [*Coira et al.*, 1982]. Rapid cooling of the Cerro Durazno at ∼320 Ma could reflect vertical movements in relation to theses basins associated with fault reactivation [*Mon and Salfity*, 1995]. The cooling differences between the Cerro Durazno and Luracatao ranges point to variable pulses of deformation and/or spatial differences in the thermal structure underneath the eastern Puna and the Eastern Cordillera. We infer the early Jurassic cooling of Cerro Durazno to be related to the onset of local extension at that time.

5.2. Cretaceous Rifting

[37] Relatively stable Ordovician to Jurassic thermal conditions ended with prerift magmatism of the continental Salta rift in the late Jurassic (∼160–150 Ma) [*Galliski and Viramonte*, 1988; *Salfity and Marquillas*, 1994]. Rifting created regional topographic gradients and a horst-and-graben crustal architecture (Figure 4) with Cretaceous sedimentary units unconformably overlying Paleozoic and Precambrian basement [*Marquillas et al.*, 2005]. Our intrusion ages of ∼160 to 150 Ma for the Fundiciones and Aguilar granites correlate with this late Jurassic magmatism. These plutons are located in the Tres Cruces branch of the Salta rift, in close proximity to older Paleozoic structures such as the SW-NE oriented Cobres lineament (Figure 4).

[38] The Jurassic-Cretaceous cooling histories differ for samples depending on their location relative to the rift structures. The western Puna (i.e., Sierra de Macón) was not influenced by Paleozoic and Mesozoic rift-related faulting and subsidence. It indicates thermally and mechanically stable crust for the western Puna. In comparison, samples from the southeastern Puna indicate rapid cooling during the prerift phase (∼153–125 Ma [*Marquillas et al.*, 2005]) and the first synrift cycle (∼125–98 Ma [*Marquillas et al.*, 2005]), likely reflecting initial faulting and tectonic subsidence in the Brealito subbasin (Figure 4). Although MDD models for the Colomé pluton and Cerro Durazno range are only weakly constrained to Cretaceous and younger ages, AFT data from these samples indicate rapid cooling during the early Cretaceous [*Deeken et al.*, 2006]. Interestingly, when combined with the AFT data, rapid cooling indicates a southward temporal trend, beginning at the Complejo Oire granite ∼164–120 Ma, then Valle de Luracatao and Colomé ∼150–100 Ma, and finally the Cerro Durazno Range 120–80 Ma. The precise age of individual rift structures is unknown, but rift-related fault displacement is the most likely cause for the rapid cooling of these intrusions. If true, these spatiotemporal variations in cooling imply that different faults were active at different times. Rapid cooling of the southern samples ceased with the end of the first synrift stage in the middle Cretaceous, probably associated with the termination of faulting [*Bianucci et al.*, 1982] and a regional modification of rift margins in the Brealito subbasin (Figure 4).

[39] In the north, the Cretaceous cooling history at Fundiciones differs substantially from the Cobres and Aguilar cooling histories. The Fundiciones granite has a pronounced alkaline geochemistry [*Viramonte et al.*, 1999], consistent with minor partial melting of a depleted subcontinental mantle [*Galliski and Viramonte*, 1988]. We interpret the fast initial rapid cooling at Fundiciones as magmatic cooling following shallow emplacement depths and initial extension. In comparison, petrological analyses show that the Aguilar pluton has subalkaline affinities [*Galliski and Viramonte*, 1988], consistent with the Cretaceous Salta rift intracratonic setting. Both the Aguilar and Cobres granites resided at temperatures >250°C until the late Cretaceous, then cooled rapidly during the latest Cretaceous to middle Paleocene (∼70–55 Ma). During this time, the Aguilar and Cobres granites were within the realm of the rift system (Figure 4) and might have been affected by thermal subsidence during the initial postrift stage (∼70–60 Ma [*Marquillas et al.*, 2005]). This interpretation is consistent with previous studies that have attributed the deposition of the late Cretaceous/early Paleogene sedimentary Balbuena group to postrift thermal subsidence [e.g., *Galliski and Viramonte*, 1988; *Grier et al.*, 1991; *Salfity and Marquillas*, 1994; *Marquillas et al.*, 2005]. However, the observed cooling could also be caused by shortening and hence reflect thrust-related crustal loading in northern Chile that induced flexural subsidence in the distal parts of the basin and overprinted the postrift thermal subsidence during the deposition of the Paleocene/Eocene Santa Barbara group [*Decelles et al.*, 2011; *Siks and Horton*, 2011].

[40] The differences in cooling histories between the Cerro Durazno and the Luracatao samples along the southeastern Puna/Eastern Cordillera transition, as well as differences between the Fundiciones and the Aguilar and Cobres granites along the northeastern Puna/Eastern Cordillera transition, suggests important differences in the timing of cooling and fault initiation/reactivation along the eastern Puna and the Eastern Cordillera. This contrast could reflect long-standing Paleozoic disparities in the crust or may be related to differences in Paleozoic lithology, sedimentary cover and/or proximity to the magmatic arc/deformation front.

5.3. Cenozoic Cooling

[41] Paleogene crustal shortening caused the compressional inversion of rift-related normal faults [*Grier et al.*, 1991; *Cristallini et al.*, 1997; *Kley and Monaldi*, 2002; *Kley et al.*, 2005]. Topographic uplift and exhumation of crustal segments at the eastern Puna/Eastern Cordillera boundary is constrained at 50 to 24 Ma by AFT data [*Andriessen and Reutter*, 1994; *Coutand et al.*, 2001; *Carrapa et al.*, 2005; *Deeken et al.*, 2006]. Our K-feldspar results help to resolve the Cenozoic cooling history for only one sample. The Aguilar granite MDD modeling shows a phase of fast cooling from 35 to 25 Ma, consistent with the AFT data (Figure 4g). For all other samples, our results constrain cooling throughout the Cenozoic to have been less than ∼150°C, the typical minimum temperature sensitivity for ^{40}Ar diffusion in K-feldspar. This implies that total

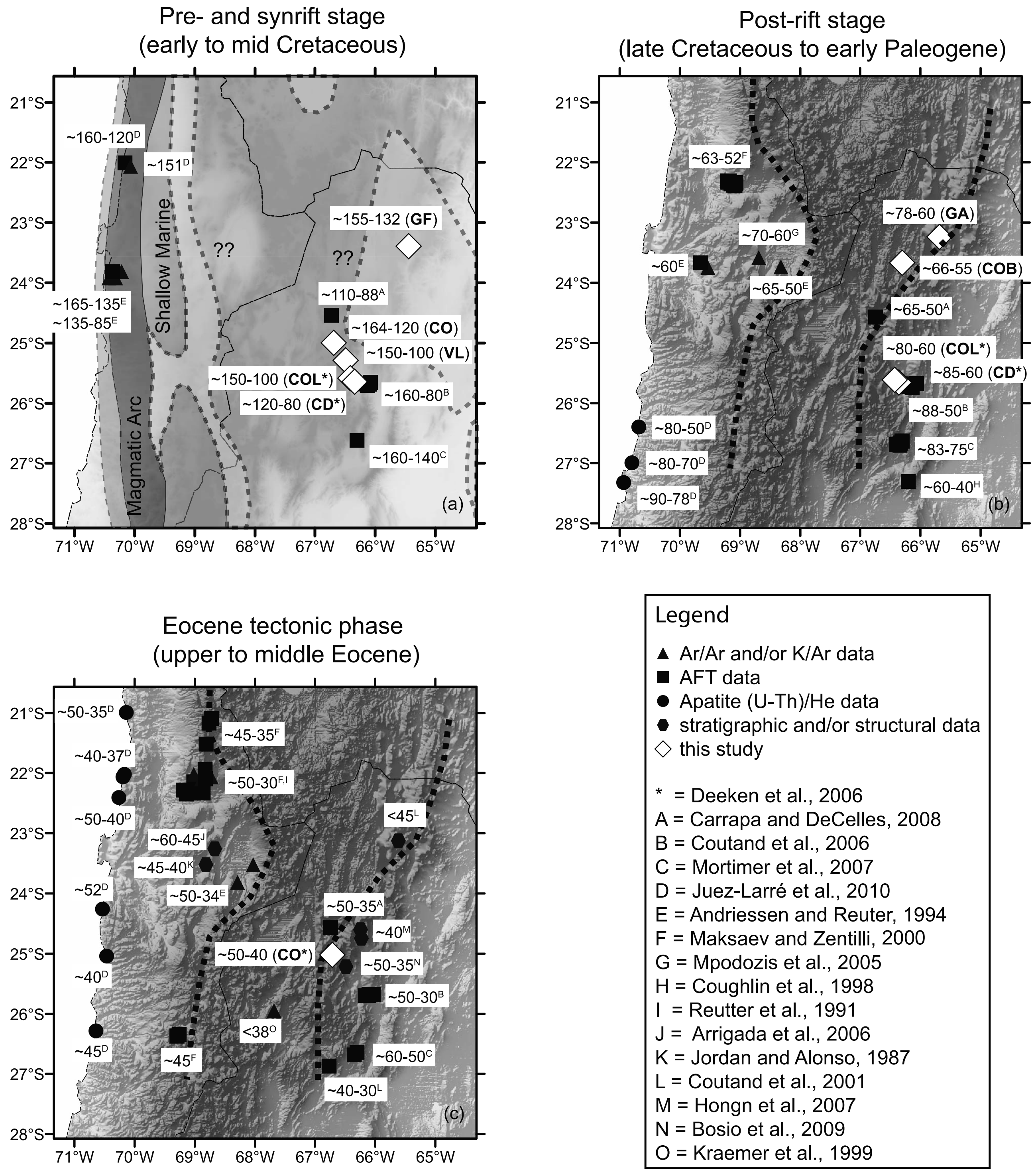

Figure 5. Shaded 30 m ASTER GDEM of the central Andes (~22°S–28°S). White diamonds represent our sample location; black symbols indicate previously published data. The numbers indicate the timing of shortening, deformation and/or enhanced cooling inferred from geothermochronology, stratigraphy, and structural data. Superscript capital letters refer to references. Parentheses refer to our individual samples, with asterisk indicating interpretation from *Deeken et al.* [2006].

Cenozoic unroofing was less than 6 km, assuming a 25°C/km geotherm.

[42] Miocene volcanic centers are concentrated on NW trending shear zones that mark long-lasting zones of lithospheric weakness [e.g., *Riller and Oncken*, 2003]. These zones with inferred strike-slip kinematics may have favored development of shallow magma chambers and eruptive centers [*Petrinovic et al.*, 1999]. Our new age determination of ~12.6 Ma for the Nevado de Acay, located along the Olacapato–El Toro lineament, is

consistent with a $\sim$15–10 Ma volcanic pulse in this region [*Petrinovic et al.*, 1999; *Kay et al.*, 2010]. The geochemical signature of the Nevado de Acay has been associated with a thin crust [*Coira et al.*, 1993] and well-defined fractional crystallization [*Petrinovic et al.*, 1999]. This suggests that geothermal gradients may have been higher than normal, and that nearby samples record less denudation than 6–4 km. This is consistent with thin ($\sim$0.2–2 km) late Miocene to Plio-Pleistocene stratigraphic sequences in that area [*Jordan and Alonso*, 1987].

6. Implications

[43] Our results indicate variable cooling histories that suggest differences in (1) the thermal gradient between the western, northeastern and southeastern Puna since the early Paleozoic and (2) the timing of regional activation/reactivation of long-lived structural discontinuities that have influenced the Cenozoic tectonic evolution of the Puna and the neighboring foreland sectors [*Hilley et al.*, 2005; *Hongn et al.*, 2007; *Strecker et al.*, 2007]. Samples of magmatic rocks from the northern Puna indicate residence at higher temperatures and/or greater crustal depth throughout the Paleozoic and Mesozoic in comparison to the southern Puna at present-day erosion levels. This temperature contrast probably persisted until the late Miocene when abundant ignimbrite volcanism in the northern Puna points to a higher degree of melting as to the south [*Kay and Coira*, 2009].

[44] In addition to detecting regional differences in the Paleozoic and Mesozoic cooling histories, our results reveal an episode of accelerated cooling focused within a narrow zone along the eastern Puna/Eastern Cordillera transition. Combining our data with available thermochronological, structural, and sedimentological data highlights synchronous rapid cooling along the present-day eastern and western Puna margins (Figures 5a and 5b). The onset of extensional tectonics in the Salta rift is recorded by cooling of the crust in the region that now comprises the eastern Puna margin during the late Jurassic and early Cretaceous. AFT analyses on rocks from the eastern Puna margin indicate old age populations of detrital grains, ranging between $\sim$158 and 100 Ma [*Coutand et al.*, 2006; *Mortimer et al.*, 2007; *Carrapa and DeCelles*, 2008], whose source region can be related to the outcropping Cretaceous strata (Figure 5a). Along the western Puna margin, K-Ar and AFT data record a rapid cooling phase between $\sim$152 and 118 Ma that has been interpreted to reflect contraction and uplift along the western central Andes (Figure 5a) [*Andriessen and Reutter*, 1994; *Juez-Larré et al.*, 2010]. Late Cretaceous to Paleogene rapid cooling correlates with thermal relaxation and cessation of rifting. Synchronous cooling recorded in AFT data along the eastern margin of the Puna indicates active tectonic deformation and exhumation during this time [e.g., *Coughlin et al.*, 1998; *Coutand et al.*, 2001; *Coutand et al.*, 2006; *Mortimer et al.*, 2007; *Carrapa et al.*, 2008], whereas late Cretaceous cooling along the western Andean margin is likely related to exhumation and eastward migration of the magmatic arc (Figure 5b) [e.g., *Kraemer et al.*, 1999; *Mpodozis et al.*, 2005; *Juez-Larré et al.*, 2010].

[45] Our K-feldspar thermal histories are not well constrained beyond the Paleogene but do place upper bounds on the total amount of Cenozoic denudation that could have occurred in the this region of the plateau at <4–6 km. The AFT analyses of our samples suggest accelerated Eocene exhumation along the eastern Puna margin [*Deeken et al.*, 2006]. In addition, Eocene deformation and exhumation has been proposed for many ranges along the eastern Puna/Eastern Cordillera. This region forms the transition to the broken foreland [e.g., *Coutand et al.*, 2001; *Coutand et al.*, 2006; *Carrapa and DeCelles*, 2008; *Bosio et al.*, 2009] and delineates the eastern border of a pronounced negative Bouguer gravity anomaly [*Tassara et al.*, 2006]. Exhumation and surface uplift are also evident along a relatively narrow region along the western Puna margin [*Jordan and Alonso*, 1987; *Reutter et al.*, 1991; *Maksaev and Zentilli*, 2000; *Arriagada et al.*, 2006] and along the coast [*Juez-Larré et al.*, 2010]. In contrast, tectonic activity during the middle Tertiary has been reported for only a few sites in the region that now forms the interior of the Puna plateau [*Kraemer et al.*, 1999].

[46] Our data document periods of accelerated cooling corresponding to distinct tectonic periods along a spatially focused region in northwestern Argentina, approximately 250 km wide. Reactivation of inherited ductile and brittle deformation zones and metamorphic fabrics in regions with variable thermal structures and differences in crustal depth juxtaposed along these features is most likely responsible for our observed differences in the chronology and magnitude of exhumation. Structures that accommodated Eocene shortening along the eastern Puna margin correlate with prestrained zones from the Cretaceous/Paleogene Salta rift system, which in turn are mainly associated with Ordovician crustal anomalies. Our thermochronologic data combined with previous studies emphasize the spatial correlation between Paleozoic orogenesis [e.g., *Mon and Hongn*, 1991; *Lucassen and Franz*, 2005; *Hongn and Riller*, 2007], late Jurassic-Cretaceous rift-related structures [e.g., *Hongn and Seggiaro*, 2001], and areas of Cenozoic mountain and plateau building. Taken together, these observations show that the Puna plateau and the adjacent eastern foreland region experienced a variable Paleozoic to early Cenozoic thermal and structural history and we suggest that this thermal and structural preconditioning, via inherited crustal anisotropies, may have influenced the modern boundaries of the Puna plateau.

7. Conclusions

[47] The Puna/Eastern Cordillera transition zone in northwest Argentina has experienced a variable Paleozoic to early Cenozoic history of cooling and exhumation. Post-crystallization cooling histories from Ordovician granites are noticeably different for samples along the northeastern compared to the southeastern Puna/Eastern Cordillera margin. Granitic basement from the western Puna eruptive belt indicates initial rapid cooling to 300°C by $\sim$420 Ma. Subsequent slow cooling to $\sim$150°C throughout the late Paleozoic and early Mesozoic ($\sim$380–200 Ma) points to protracted crustal residence from 8 to 4? km depths (assuming a geothermal gradient of 35°C/km) during this time, and suggests the establishment and persistence of a relatively stable thermal regime following earlier Ordovician tectonism and magmatism.

[48] In contrast, granitoids from the eastern Puna eruptive belt and the Eastern Cordillera resided at deeper crustal levels (>8 km) throughout Paleozoic and Mesozoic time. These areas experienced two phases of rapid cooling associated with rifting stages of the Salta rift: (1) Samples from the southeastern Puna margin indicate rapid cooling in the late Jurassic–early Cretaceous (~160–100 Ma), likely reflecting initial faulting and tectonic subsidence in the Brealito subbasin. (2) Northeastern Puna margin samples cooled rapidly during the latest Cretaceous to middle Paleocene (~78–55 Ma), likely reflecting thermal subsidence during the initial postrift stage. Variable cooling histories between the southeastern and northeastern Puna/Eastern Cordillera transition, as well as differences between individual samples within these domains, imply regional variations in the thermal and structural regimes characterized by nonuniform timing of cooling and fault initiation/reactivation. The pre-Cenozoic thermal and mechanical boundaries (i.e., Ordovician thermal anomalies and Cretaceous rift-related faulting) determined the documented regional pluton exhumation histories, and may have had an influence on the horizontal dimensions of the modern Puna plateau.

[49] Our results suggest that confining the Paleozoic to Mesozoic thermal and mechanical state of the Andean crust leading up to formation of the Cenozoic Puna plateau is important for establishing the initial conditions for orogenic plateau growth. Our results constrain cooling throughout the Cenozoic to have been less than ~150°C, the typical minimum temperature sensitivity for ^{40}Ar diffusion in K-feldspar. This implies that total Cenozoic unroofing was <6 km assuming a 25°C/km geotherm.

[50] **Acknowledgments.** This study was supported by the Deutsche Forschungsgemeinschaft (DFG) Andes Working Group SFB 267 (Deformationsprozesse in den Anden). We particularly thank R. Alonso for invaluable logistical help and discussions on the geology of the Puna and J. Glodny for help with mineral separations. Analyses were performed at the ion microprobe facility at UCLA, which is partly supported by a grant from the Instrumentation and Facilities Program, Division of Earth Sciences, National Science Foundation. We would also like to thank Anke Deeken and Taylor Schildgen for discussions and Suzanne Kay and an anonymous reviewer for insightful reviews that helped to focus an earlier version of this manuscript.

References

Alasino, P. H., J. A. Dahlquist, R. J. Pankhurst, C. Galindo, C. Casquet, C. W. Rapela, M. A. Larrovere, and C. M. Fanning (2012), Early Carboniferous sub- to mid-alkaline magmatism in the Eastern Sierras Pampeanas, NW Argentina: A record of crustal growth by the incorporation of mantle-derived material in an extensional setting, *Gondwana Res.*, *22*, 992–1008, doi:10.1016/j.gr.2011.12.011.

Allmendinger, R. W. (1986), Tectonic development, southeastern border of the Puna plateau, northwestern Argentine Andes, *Geol. Soc. Am. Bull.*, *97*(9), 1070–1082, doi:10.1130/0016-7606(1986)97<1070:TDSBOT>2.0.CO;2.

Allmendinger, R. W., V. A. Ramos, T. E. Jordan, M. Palma, and B. L. Isacks (1983), Paleogeography and Andean structural geometry, northwest Argentina, *Tectonics*, *2*(1), 1–16, doi:10.1029/TC002i001p00001.

Allmendinger, R. W., M. R. Strecker, J. E. Eremchuk, and P. Francis (1989), Neotectonic deformation of the southern Puna plateau, northwestern Argentina, *J. South Am. Earth Sci.*, *2*, 111–130, doi:10.1016/0895-9811(89)90040-0.

Allmendinger, R. W., T. E. Jordan, S. M. Kay, and B. L. Isacks (1997), The evolution of the Altiplano-Puna plateau of the central Andes, *Annu. Rev. Earth Planet. Sci.*, *25*, 139–174, doi:10.1146/annurev.earth.25.1.139.

Alonso, R., J. G. Viramonte, and R. Gutierrez (1985), Puna Austral—Bases para el subprovincialismo gelógico de la Puna Argentina, paper presented at IX Congreso Geologico Argentino, Asoc. Geol. Argent., Buenos Aires.

Andriessen, P. A. M., and K. J. Reutter (1994), K-Ar and fission track mineral age determination of igneous rocks related to multiple magmatic arc systems along the 23°S latitude of Chile and NW Argentina, in *Tectonics of the Southern Central Andes*, edited by K. J. Reutter, E. Scheuber, and P. J. Wigger, pp. 141–153, Springer, Berlin.

Arriagada, C., P. R. Cobbold, and P. Roperch (2006), Salar de Atacama basin: A record of compressional tectonics in the central Andes since the mid-Cretaceous, *Tectonics*, *25*, TC1008, doi:10.1029/2004TC001770.

Babeyko, A. Y., and S. V. Sobolev (2005), Quantifying different modes of the late Cenozoic shortening in the central Andes, *Geology*, *33*(8), 621–624, doi:10.1130/G21126.1.

Bahlburg, H. (1990), *The Ordovician Basin in the Puna of NW Argentina and N Chile: Geodynamic Evolution From Back-Arc to Foreland Basin*, *Geotekt. Forsch.*, vol. 75, 107 pp., Schweizerbart, Stuttgart, Germany.

Bahlburg, H., and K. P. Furlong (1996), Lithospheric modeling of the Ordovician foreland basin in the Puna of northwestern Argentina: On the influence of arc loading on foreland basin formation, *Tectonophysics*, *259*, 245–258, doi:10.1016/0040-1951(95)00129-8.

Bahlburg, H., and F. Herve (1997), Geodynamic evolution and tectonostratigraphic terranes of northwestern Argentina and northern Chile, *Geol. Soc. Am. Bull.*, *109*(7), 869–884, doi:10.1130/0016-7606(1997)109<0869:GEATTO>2.3.CO;2.

Becchio, R., F. Lucassen, S. Kaseman, G. Franz, and J. Viramonte (1999), Geoquímica y sistemática isotópica de rocas metamórficas del Paleozoic inferior. Noroeste de Argentina y Norte de Chile (21°–27°S), *Acta Geol. Hisp.*, *34*, 273–299.

Bianucci, H., J. F. Homovc, and O. M. Acevedo (1982), Inversion tectonica y plegamientos resultantes en la comarca Puesto Guardian—Dos Puntitas, Departamento de Oran, Provincia de Salta, paper presented at 1st Congreso Nacional de Hidrocarburos, Petroleo y Gas, Exploracion, Inst. Argent. Petrol., Buenos Aires.

Bosio, P. P., J. Powell, C. del Papa, and F. Hongn (2009), Middle Eocene deformation-sedimentation in the Luracatao Valley: Tracking the beginning of the foreland basin of northwestern Argentina, *J. South Am. Earth Sci.*, *28*, 142–154, doi:10.1016/j.jsames.2009.06.002.

Büttner, S. H., J. Glodny, F. Lucassen, K. Wemmer, S. Erdmann, R. Handler, and G. Franz (2005), Ordovician metamorphism and plutonism in the Sierra de Quilmes metamorphic complex: Implications for the tectonic setting of the northern Sierras Pampeanas (NW Argentina), *Lithos*, *83*(1–2), 143–181, doi:10.1016/j.lithos.2005.01.006.

Carrapa, B., and P. G. DeCelles (2008), Eocene exhumation and basin development in the Puna of northwestern Argentina, *Tectonics*, *27*, TC1015, doi:10.1029/2007TC002127.

Carrapa, B., D. Adelmann, G. E. Hilley, E. Mortimer, E. R. Sobel, and M. R. Strecker (2005), Oligocene range uplift and development of plateau morphology in the southern central Andes, *Tectonics*, *24*, TC4011, doi:10.1029/2004TC001762.

Carrapa, B., M. R. Strecker, and E. R. Sobel (2006), Cenozoic orogenic growth in the central Andes: Evidence from sedimentary rock provenance and apatite fission track thermochronology in the Fiambala Basin, southernmost Puna plateau margin (NW Argentina), *Earth Planet. Sci. Lett.*, *247*, 82–100, doi:10.1016/j.epsl.2006.04.010.

Carrapa, B., P. G. Decelles, P. W. Reiners, G. Gehrels, and A. Biswas (2008), Exhumation and basin evolution of the Puna plateau of NW Argentina revealed by a multi geo-thermochronological approach, *Geochim. Cosmochim. Acta*, *72*(12), A139.

Carrapa, B., P. G. DeCelles, P. W. Reiners, G. E. Gehrels, and M. Sudo (2009), Apatite triple dating and white mica ^{40}Ar/^{39}Ar thermochronology of syntectonic detritus in the central Andes: A multiphase tectonothermal history, *Geology*, *37*(5), 407–410, doi:10.1130/G25698A.1.

Carrera, N., and J. A. Muñoz (2008), Thrusting evolution in the southern Cordillera Oriental (northern Argentine Andes): Constraints from growth strata, *Tectonophysics*, *459*, 107–122, doi:10.1016/j.tecto.2007.11.068.

Carrera, N., J. A. Muñoz, F. Sàbat, R. Mon, and E. Roca (2006), The role of inversion tectonics in the structure of the Cordillera Oriental (NW Argentinean Andes), *J. Struct. Geol.*, *28*, 1921–1932, doi:10.1016/j.jsg.2006.07.006.

Casquet, C., R. J. Pankhurst, C. W. Rapela, C. Galindo, J. Dahlquist, E. Baldo, J. Saavedra, J. M. Gonzalez Casado, and C. M. Fanning (2005), Grenvillian massif-type anorthosites in the Sierras Pampeanas, *J. Geol. Soc.*, *162*(1), 9–12, doi:10.1144/0016-764904-100.

Cladouhos, T. T., R. W. Allmendinger, B. Coira, and E. Farrar (1994), Late Cenozoic deformation in the central Andes: Fault kinematics from the northern Puna, northwestern Argentina and southwestern Bolivia, *J. South Am. Earth Sci.*, *7*, 209–228, doi:10.1016/0895-9811(94)90008-6.

Coira, B., J. Davidson, C. Mpodozis, and V. Ramos (1982), Tectonic and magmatic evolution of the Andes of northern Argentina and Chile, in *Earth Sci. Rev.*, *18*, 303–332, doi:10.1016/0012-8252(82)90042-3.

Coira, B., S. M. Kay, and J. Viramonte (1993), Upper Cenozoic magmatic evolution of the Argentine Puna: A model for changing subduction geometry, *Int. Geol. Rev.*, *35*, 677–720, doi:10.1080/00206819309465552.

Coira, B., S. M. Kay, B. Perez, B. Woll, M. Hanning, and P. Flores (1999), Magmatic sources and tectonic setting of Gondwana margin Ordovician magmas, northern Puna of Argentina and Chile, *Spec. Pap. Geol. Soc. Am.*, *336*, 145–170.

Coira, B., M. Koukharsky, S. Ribeiro Guevara, and C. E. Cisterna (2009a), Puna (Argentina) and northern Chile Ordovician basic magmatism: A contribution to the tectonic setting, *J. South Am. Earth Sci.*, *27*, 24–35, doi:10.1016/j.jsames.2008.10.002.

Coira, B., A. Kirschbaum, F. Hongn, B. Perez, and N. Menegatti (2009b), Basic magmatism in northeastern Puna, Argentina: Chemical composition and tectonic setting in the Ordovician back-arc, *J. South Am. Earth Sci.*, *28*, 374–382, doi:10.1016/j.jsames.2009.04.007.

Coughlin, T. J., P. B. O'Sullivan, B. P. Kohn, and R. J. Holcombe (1998), Apatite fission-track thermochronology of the Sierras Pampeanas, central western Argentina: Implications for the mechanism of plateau uplift in the Andes, *Geology*, *26*(11), 999–1002, doi:10.1130/0091-7613(1998)026<0999:AFTTOT>2.3.CO;2.

Coutand, I., P. Gautier, P. R. Cobbold, M. de Urreiztieta, A. Chauvin, D. Gapais, E. A. Rossello, and O. Lopez-Gammundi (2001), Style and history of Andean deformation, Puna plateau, northwestern Argentina, *Tectonics*, *20*(2), 210–234, doi:10.1029/2000TC900031.

Coutand, I., B. Carrapa, A. Deeken, A. K. Schmitt, E. R. Sobel, and M. R. Strecker (2006), Propagation of orographic barriers along an active range front; insights from sandstone petrography and detrital apatite fission-track thermochronology in the intramontane Angastaco Basin, NW Argentina, *Basin Res.*, *18*(1), 1–26, doi:10.1111/j.1365-2117.2006.00283.x.

Cristallini, E., A. H. Cominguez, and V. A. Ramos (1997), Deep structure of the Metan-Guachipas region; tectonic inversion in northwestern Argentina, *J. South Am. Earth Sci.*, *10*, 403–421, doi:10.1016/S0895-9811(97)00026-6.

Cristiani, C., M. Matteini, R. Mazzuoli, R. Omarini, and I. M. Villa (2005), Petrology of late Jurassic-early Cretaceous Tusaquillas and Abra Laite-Aguilar plutonic complexes (central Andes, 23°05′S–66°05′W): A comparison with rift-related magmatism of NW Argentina and E Bolvia, in *Mesozoic to Cenozoic Alkaline Magmatism in the Brazilian Platform*, edited by P. Comin-Chiaramonti, pp. 213–240, Edusp/Fapesp, São Paulo.

Dahlquist, J. A., R. J. Pankhurst, C. W. Rapela, C. Casquet, C. M. Fanning, P. H. Alasino, and M. Baez (2006), The San Blas Pluton: An example of Carboniferous plutonism in the Sierra Pampeanas, Argentina, *J. South Am. Earth Sci.*, *20*, 341–350, doi:10.1016/j.jsames.2005.08.006.

Dahlquist, J. A., P. H. Alasino, G. N. Eby, C. Galindo, and C. Casquet (2010), Fault controlled Carboniferous A-type magmatism in the proto-Andean foreland (Sierra Pampeanas, Argentina): Geochemical constraints and petrogenesis, *Lithos*, *115*, 65–81, doi:10.1016/j.lithos.2009.11.006.

Damm, K. W., S. Pichowiak, R. S. Harmon, W. Todt, S. Kelley, R. Omarini, and H. Niemeyer (1990), Pre-Mesozoic evolution of the central Andes: The basement revisited, *Spec. Pap. Geol. Soc. Am.*, *241*, 101–126.

Decelles, P. G., B. Carrapa, B. K. Horton, and G. E. Gehrels (2011), Cenozoic foreland basin system in the central Andes of northwestern Argentina: Implications for Andean geodynamics and modes of deformation, *Tectonics*, *30*, TC6013, doi:10.1029/2011TC002948.

Deeken, A., E. R. Sobel, M. R. Haschke, and U. Riller (2005), Age of initiation and growth pattern of the Puna plateau, NW-Argentina, constrained by AFT thermochtonology, paper presented at 19th Colloquium on Latin American Geosciences, GeoForschungsZentrum Potsdam, Potsdam, Germany, 18–20 April.

Deeken, A., E. R. Sobel, I. Coutand, M. Haschke, U. Riller, and M. R. Strecker (2006), Development of the southern Eastern Cordillera, NW Argentina, constrained by apatite fission track thermochronology: From early Cretaceous extension to middle Miocene shortening, *Tectonics*, *25*, TC6003, doi:10.1029/2005TC001894.

Ege, H., E. R. Sobel, E. Scheuber, and V. Jacobshagen (2007), Exhumation history of the southern Altiplano plateau (southern Bolivia) constrained by apatite fission-track thermochronology, *Tectonics*, *26*, TC1004, doi:10.1029/2005TC001869.

Elger, K., O. Oncken, and J. Glodny (2005), Plateau-style accumulation of deformation: Southern Altiplano, *Tectonics*, *24*, TC4020, doi:10.1029/2004TC001675.

Fielding, E., B. Isacks, M. Barazangi, and C. Duncan (1994), How flat is Tibet, *Geology*, *22*(2), 163–167, doi:10.1130/0091-7613(1994)022<0163:HFIT>2.3.CO;2.

Galliski, M. A., and J. G. Viramonte (1988), The Cretaceous paleorift in northwestern Argentina: A petrologic approach, *J. South Am. Earth Sci.*, *1*, 329–342, doi:10.1016/0895-9811(88)90021-1.

Grier, M. E., J. A. Salfity, and R. W. Allmendinger (1991), Andean reactivation of the Cretaceous Salta Rift, northwestern Argentina, *J. South Am. Earth Sci.*, *4*, 351–372, doi:10.1016/0895-9811(91)90007-8.

Grissom, G. C., S. M. Debari, and L. W. Snee (1998), Geology of the Sierra de Fiambalá, northwestern Argentina: Implications for Early Palaeozoic Andean tectonics, *Geol. Soc. Spec. Publ.*, *142*, 297–323, doi:10.1144/GSL.SP.1998.142.01.15.

Grosse, P., F. Soellner, M. A. Báez, A. J. Toselli, J. N. Rossi, and J. D. de la Rosa (2009), Lower Carboniferous post-orogenic granites in central-eastern Sierra de Velasco, Sierras Pampeanas, Argentina: U-Pb monzanite geochronology, geochemistry and Sr-Nd isotopes, *Int. J. Earth Sci.*, *98*, 1001–1025, doi:10.1007/s00531-007-0297-5.

Halpern, M., and C. O. Latorre (1973), Estudio geochronologico inicial de rocas del noroeste de la Republica Argentina, *Asoc. Geol. Argent. Rev.*, *28*(2), 195–205.

Harrison, T. M., M. T. Heizler, and O. M. Lovera (1993), In vacuo crushing experiments and K-feldspar thermochronometry, *Earth Planet. Sci. Lett.*, *117*(1–2), 169–180, doi:10.1016/0012-821X(93)90124-R.

Harrison, T. M., M. T. Heizler, O. M. Lovera, W. Chen, and M. Grove (1994), A chlorine disinfectant for excess argon released from K-feldspar during step heating, *Earth Planet. Sci. Lett.*, *123*(1–3), 95–104, doi:10.1016/0012-821X(94)90260-7.

Harrison, T. M., Y. An, M. Grove, O. M. Lovera, F. J. Ryerson, and X. Zhou (2000), The Zedong Window: A record of superposed Tertiary convergence in southeastern Tibet, *J. Geophys. Res.*, *105*(B8), 19,211–19,230, doi:10.1029/2000JB900078.

Harrison, T. M., M. Grove, O. M. Lovera, and P. K. Zeitler (2005), Continuous thermal histories from inversion of closure profiles, *Rev. Mineral. Geochem.*, *58*(1), 389–409, doi:10.2138/rmg.2005.58.15.

Hatzfeld, D., and P. Molnar (2010), Comparisons of the kinematics and deep structures of the Zagros and Himalaya and of the Iranian and Tibetan Plateaus and geodynamic implications, *Rev. Geophys.*, *48*, RG2005, 10.1029/2009RG000304.

Henry, S. G., and H. N. Pollack (1988), Terrestrial heat flow above the Andean Subduction Zone in Bolivia and Peru, *J. Geophys. Res.*, *93*(B12), 15,153–15,162, doi:10.1029/JB093iB12p15153.

Hilley, G. E., P. M. Blisniuk, and M. R. Strecker (2005), Mechanics and erosion of basement-cored uplift provinces, *J. Geophys. Res.*, *110*, B12409, doi:10.1029/2005JB003704.

Höckenreiner, M., F. Soellner, and H. Miller (2003), Dating the TIPA shear zone: An early Devonian terrane boundary between the Famatian and Pampean systems (NW Argentina), *J. South Am. Earth Sci.*, *16*, 45–66, doi:10.1016/S0895-9811(03)00018-X.

Hongn, F. D., and R. Mon (1999), La deformación ordovícica en el borde oriental de la Puna, in *Geología del Noroeste Argentino, Relatorio XIV Congreso Geológico Argentino*, vol. 1, edited by G. González Bonorino et al., pp. 212–216, Univ. Nac. de Salta, Salta, Argentina.

Hongn, F. D., and U. Riller (2007), Tectonic evolution of the western margin of Gondwana inferred from syntectonic emplacement of Paleozoic granitoid plutons in northwest Argentina, *J. Geol.*, *115*(2), 163–180, doi:10.1086/510644.

Hongn, F., and R. E. Seggiaro (2001), Hoja geológica 2566-III, Cachi, *Bol. 248*, scale 1:250,000, Serv. Geol. Minero Argent., Buenos Aires.

Hongn, F., A. Aranguren, J. M. Tubia, and R. Mon (1999), Estructura, fábrica magnética y emplazamiento de los granitos de Brealito y La Paya, basamento del valle Calchaquí, Saltam Argentina, *Acta Geol. Hisp.*, *34*, 301–317.

Hongn, F., C. del Papa, J. Powell, I. Petrinovic, R. Mon, and V. Deraco (2007), Middle Eocene deformation and sedimentation in the Puna-Eastern Cordillera transition (23°–26°S): Control by preexisting heterogeneities on the pattern of initial Andean shortening, *Geology*, *35*(3), 271–274, doi:10.1130/G23189A.1.

Hongn, F. D., J. M. Tubia, A. Aranguren, N. Vegas, R. Mon, and G. R. Dunning (2010), Magmatism coeval with lower Paleozoic shelf basins in NW-Argentina (Tastil batholith): Constraints on current stratigraphic and tectonic interpretations, *J. South Am. Earth Sci.*, *29*, 289–305, doi:10.1016/j.jsames.2009.07.008.

Isacks, B. L. (1988), Uplift of the central Andean Plateau and bending of the Bolivian Orocline, *J. Geophys. Res.*, *93*(B4), 3211–3231, doi:10.1029/JB093iB04p03211.

Jordan, T. E., and R. N. Alonso (1987), Cenozoic stratigraphy and basin tectonics of the Andes Mountains, 20°–28° south latitude, *AAPG Bull.*, *71*(1), 49–64.

Juez-Larré, J., N. Kukowski, T. J. Dunai, A. J. Hartley, and P. A. M. Andriessen (2010), Thermal and exhumation history of the Coastal

Cordillera arc of northern Chile revealed by thermochronological dating, *Tectonophysics*, *495*, 48–66, doi:10.1016/j.tecto.2010.06.018.
Kay, S. M., and B. L. Coira (2009), Shallowing and steepening subduction zones, continental lithospheric loss, magmatism, and crustal flow under the central Andean Altiplano-Puna plateau, *Geol. Soc. Am. Mem.*, *204*, 229–259, doi:10.1130/2009.1204(11).
Kay, S. M., B. Coira, and J. Viramonte (1994), Young mafic back arc volcanic rocks as indicators of continental lithospheric delamination beneath the Argentine Puna plateau, central Andes, *J. Geophys. Res.*, *99*, 24,323–24,339, doi:10.1029/94JB00896.
Kay, S. M., B. L. Coira, P. J. Caffe, and C.-H. Chen (2010), Regional chemical diversity, crustal and mantle sources and evolution of central Andean Puna plateau ignimbrites, *J. Volcanol. Geotherm. Res.*, *198*, 81–111, doi:10.1016/j.jvolgeores.2010.08.013.
Kirschbaum, A., F. Hongn, and N. Menegatti (2006), The Cobres Plutonic Complex, eastern Puna (NW Argentina): Petrological and structural constraints for Lower Paleozoic magmatism, *J. South Am. Earth Sci.*, *21*, 252–266, doi:10.1016/j.jsames.2006.04.003.
Kleine, T., K. Mezger, U. Zimmermann, C. Münker, and H. Bahlburg (2004), Crustal evolution along the Early Ordovician Proto-Andean margin of Gondwana: Trace element and isotope evidence from the Complejo Igneo Pocitos (northwest Argentina), *J. Geol.*, *112*, 503–520, doi:10.1086/422663.
Kley, J. (1996), Transition from basement-involved to thin-skinned thrusting in the Cordillera Oriental of southern Bolivia, *Tectonics*, *15*, 763–775, doi:10.1029/95TC03868.
Kley, J., and C. R. Monaldi (2002), Tectonic inversion in the Santa Barbara System of the central Andean foreland thrust belt, northwestern Argentina, *Tectonics*, *21*(6), 1061, doi:10.1029/2002TC902003.
Kley, J., C. R. Monaldi, and J. A. Salfity (1999), Along-strike segmentation of the Andean foreland; causes and consequences, *Tectonophysics*, *301*, 75–94, doi:10.1016/S0040-1951(98)90223-2.
Kley, J., E. A. Rossello, C. R. Monaldi, and B. Habighorst (2005), Seismic and field evidence for selective inversion of Cretaceous normal faults, Salta Rift, northwest Argentina, *Tectonophysics*, *399*, 155–172, doi:10.1016/j.tecto.2004.12.020.
Koukharsky, M., S. Quenardelle, V. D. Litvak, S. Page, and E. B. Maisonnave (2002), Plutonismo del Ordovicico inferior en el sector norte de la sierra de Macon, provincia de Salta, *Asoc. Geol. Argent. Rev.*, *57*(2), 173–181.
Kraemer, B., D. Adelmann, M. Alten, W. Schnurr, K. Erpenstein, E. Kiefer, P. van den Bogaard, and K. Gorler (1999), Incorporation of the Paleogene foreland into the Neogene Puna plateau: The Salar de Antofalla area, NW Argentina, *J. South Am. Earth Sci.*, *12*, 157–182, doi:10.1016/S0895-9811(99)00012-7.
Linares, E. (1979), Catalogo de edades radiometricas determinadas para la Republica Argentina y catalogode edades radiometricas realizadaspor ingeis y sin publicar, *Asoc. Geol. Ar., Pub. Esp. Ser.*, *B6*, 32 pp.
Llambias, J. K., A. M. Sato, and J. Tomsic (1985), Geologia y caracteristicas quimicas del stock terciario del Nevado de Acay y vulcanitas asociadas, provincia de Salta, *Asoc. Geol. Argent. Rev.*, *40*(3–4), 158–175.
Lork, A., and H. Bahlburg (1993), Precise U-Pb ages of monazites from the Faja Eruptiva de la Puna Oriental, and the Cordillera Oriental, NW Argentina, in *Geología y Recursos Naturales de Mendoza: 12° Congreso Geológico Argentino y 2° Congreso de Exploración de Hidrocarburos, Mendoza, Actas 4*, edited by V. A. Ramos, pp. 1–6, La Comisión, Buenos Aires.
Lovera, O. M., F. M. Richter, and T. M. Harrison (1989), The $^{40}Ar/^{39}Ar$ thermochronometry for slowly cooled samples having a distribution of diffusion domain sizes, *J. Geophys. Res.*, *94*(B12), 17,917–17,935.
Lovera, O. M., M. Grove, T. M. Harrison, and K. I. Mahon (1997), Systematic analysis of K-feldspar $^{40}Ar/^{39}Ar$ step heating results: I. Significance of activation energy determinations, *Geochim. Cosmochim. Acta*, *61*(15), 3171–3192, doi:10.1016/S0016-7037(97)00147-6.
Lovera, O. M., M. Grove, and T. M. Harrison (2002), Systematic analysis of K-feldspar $^{40}Ar/^{39}Ar$ step heating results: II. Relevance of laboratory argon diffusion properties to nature, *Geochim. Cosmochim. Acta*, *66*(7), 1237–1255, doi:10.1016/S0016-7037(01)00846-8.
Lucassen, F., and G. Franz (2005), The early Palaeozoic Orogen in the central Andes: A non-collisional orogen comparable to the Cenozoic high plateau?, *Geol. Soc. Spec. Publ.*, *246*, 257–273, doi:10.1144/GSL.SP.2005.246.01.09.
Lucassen, F., H. G. Wilke, J. Viramonte, R. Becchio, G. Franz, A. Laber, K. Wemmer, and P. Vroon (1996), The Paleozoic basement of the central Andes (18°–26°S). A metamorphic view, paper presented at 3rd International Symposium on Andean Geodynamics, Univ. Rennes 1, St. Malo, France
Lucassen, F., R. Becchio, H. G. Wilke, M. F. Thirwall, J. Viramonte, G. Franz, and K. Wemmer (2000), Proterozoic-Paleozoic development of the basement of the central Andes (18°–26°S): A mobile belt of the South American craton, *J. South Am. Earth Sci.*, *13*, 697–715, doi:10.1016/S0895-9811(00)00057-2.
Lucassen, F., R. Harmon, G. Franz, R. L. Romer, R. Becchio, and W. Siebel (2002), Lead evolution of the Pre-Mesozoic crust in the central Andes (18–27°): Progressive homogenisation of Pb, *Chem. Geol.*, *186*, 183–197, doi:10.1016/S0009-2541(01)00407-7.
Mahon, K. I. (1996), The new "York" regression: Application of an improved statistical method to geochemistry, *Int. Geol. Rev.*, *38*(4), 293–303, doi:10.1080/00206819709465336.
Maksaev, V. (1990), Metallogeny, geological evolution, and thermochronology of the Chilean Andes between latitudes 21° and 26° south, and the origin of the major porphyry copper deposits, PhD thesis, 555 pp., Dalhouse Univ., Halifax, Nova Scotia, Canada.
Maksaev, V., and M. Zentilli (2000), Fission track thermochronology of the Domeyko Cordillera, northern Chile: Implications for Andean tectonics and porphyry copper metallogenesis, *Explor. Min. Geol.*, *8*(1–2), 65–89.
Marquillas, R. A., C. del Papa, and I. F. Sabino (2005), Sedimentary aspects and paleoenvironmental evolution of a rift basin; Salta Group, Cretaceous-Paleogene, northwestern Argentina, *Int. J. Earth Sci.*, *94*(1), 94–113, doi:10.1007/s00531-004-0443-2.
Marrett, R. A., R. W. Allmendinger, R. Alonso, and R. E. Drake (1994), Late Cenozoic tectonic evolution of the Puna plateau and adjacent foreland, northwestern Argentine Andes, *J. South Am. Earth Sci.*, *7*, 179–207, doi:10.1016/0895-9811(94)90007-8.
Mazzuoli, R., et al. (2008), Miocene magmatism and tectonics of the easternmost sector of the Calama–Olacapato–El Toro fault system in central Andes at ∼24°S: Insights into the evolution of the Eastern Cordillera, *Geol. Soc. Am. Bull.*, *120*(11–12), 1493–1517, doi:10.1130/B26109.1.
McDougall, I., and T. M. Harrison (1999), *Geochronology and Thermochronology by the $^{40}Ar/^{39}Ar$ Method*, 269 pp., Oxford Univ. Press, New York,.
Méndez, V., A. Navarini, D. Plaza, and V. Viera (1973), Faja eruptiva de la Puna oriental, *Actas Jorn. Geol. Argent.*, *5*(4), 89–100.
Mirre, J. C. (1974), El granito del Acay, intrusivo de edad terciaria en el ambiente de Puna, *Asoc. Geol. Argent. Rev.*, *29*(2), 205–212.
Mon, R., and F. Hongn (1991), The structure of the Precambrian and lower Paleozoic basement of the central Andes between 22° and 32°S. Lat, *Geol. Rundsch.*, *80*(3), 745–758, doi:10.1007/BF01803699.
Mon, R., and J. A. Salfity (1995), Tectonic evolution of the Andes of northern Argentina, *AAPG Mem.*, *62*, 269–283.
Mon, R., C. R. Monaldi, and J. A. Salfity (2005), Curved structures and interference fold patterns associated with lateral ramps in the Eastern Cordillera, central Andes of Argentina, *Tectonophysics*, *399*, 173–179, doi:10.1016/j.tecto.2004.12.021.
Mortimer, E., B. Carrapa, I. Coutand, L. Schoenbohm, E. R. Sobel, and J. S. Gomez (2007), Fragmentation of a foreland basin in response to out-of-sequence basement uplifts and structural reactivation: El Cajon-Campo del Arenal basin, NW Argentina, *Geol. Soc. Am. Bull.*, *119*(5–6), 637–653, doi:10.1130/B25884.1.
Mpodozis, C., F. Hervé, J. Davidson, and C. González (1983), Los granitoides de Cerro de Lila, manifestaciones de un episodio intrusivo y termal del Paleozoico inferior en los Andes del N de Chile. Santiago, Chile, *Rev. Geol. Chile*, *18*, 3–14.
Mpodozis, C., C. Arriagada, M. Basso, P. Roperch, P. Cobbold, and M. Reich (2005), Late Mesozoic to Paleogene stratigraphy of the Salar de Atacama Basin, Antofagasta, northern Chile: Implications for the tectonic evolution of the central Andes, *Tectonophysics*, *399*, 125–154, doi:10.1016/j.tecto.2004.12.019.
Omarini, R., J. G. Viramonte, U. Cordani, J. A. Salfity, and K. Kawashita (1984), Estudio geocronológico Rb-SR de la Faja Eruptiva de la Puna en el sector de San Antonio de los Cobres, provincia de Salta, paper presented at V Congreso Geológico Argentino, Salta, Argentina.
Oncken, O., D. Hindle, J. Kley, K. Elger, P. Victor, and K. Schemmann (2006), Deformation of the central Andean upper plate system: Facts, fiction, and constraints for plateau models, in *The Andes: Active Subduction Orogeny*, edited by O. Oncken et al., pp. 3–27, Springer, Berlin, doi:10.1007/978-3-540-48684-8_1.
Otamendi, J. E., L. P. Pinotti, M. A. S. Basei, and A. M. Tibaldi (2010), Evaluation of petrogenetic models for intermediate and silicic plutonic rocks from the Sierra de Valle Fértil-La Huerta, Argentina: Petrologic constraints on the origin of igneous rocks in the Ordovician Famatinian-Puna paleoarc, *J. South Am. Earth Sci.*, *30*, 29–45, doi:10.1016/j.jsames.2010.07.004.
Palma, M. A., P. Parica, and V. A. Ramos (1986), El granito Archibarca: Su edad y significado tectónico, provincia de Catamarca, *Asoc. Geol. Argent. Rev.*, *41*(3–4), 414–419.
Pankhurst, R. J., C. W. Rapela, and C. M. Fanning (2000), Age and origin of coeval TTG, I- and S-type granites in the Famatinian Belt of the NW Argentina, *Trans. R. Soc. Edinburgh Earth Sci.*, *91*, 151–168.

Parsons, I., W. L. Brown, and J. V. Smith (1999), $^{40}Ar/^{39}Ar$ thermochronology using alkali feldspars: Real thermal history or mathematical mirage of microtexture?, *Contrib. Mineral. Petrol.*, *136*, 92–110, doi:10.1007/s004100050526.
Pearson, D. M., P. Kapp, P. W. Reiners, G. E. Gehrels, M. N. Ducea, A. Pullern, J. E. Otamendi, and R. N. Alonso (2012), Major Miocene exhumation by fault-propagation folding within a metamorphosed, early Paleozoic thrust belt: Northwestern Argentina, *Tectonics*, *31*, TC4023, doi:10.1029/2011TC003043.
Petrinovic, I. A., J. Mitjavila, J. G. Viramonte, J. Martí, R. Becchio, M. Arnosio, and F. Colombo (1999), Descripción geoquímica y geocronológica de secuencias volcánicas neógenas de Trasarco, en el extremo oriental de la Cadena Volcánica Transversal del Quevar (Noroeste de Argentina), *Acta Geol. Hisp.*, *34*, 255–273.
Poma, S., S. Quenardelle, V. Litvak, E. B. Maisonnave, and M. Koukharsky (2004), The Sierra de Macon, plutonic expression of the Ordovician magmatic arc, Salta Province, Argentina, *J. South Am. Earth Sci.*, *16*, 587–597, doi:10.1016/j.jsames.2003.10.002.
Quidelleur, X., M. Grove, O. Lovera, T. Harrison, and A. Yin (1997), Thermal evolution and slip history of the Renbu Zedong Thrust, southeastern Tibet, *J. Geophys. Res.*, *102*(B2), 2659–2679.
Ramos, V. A. (2008), The basement of the central Andes: The Arequipa and related terranes, *Annu. Rev. Earth Planet. Sci.*, *36*, 289–324, doi:10.1146/annurev.earth.36.031207.124304.
Rapela, C. W., A. J. Toselli, L. Heaman, and J. Saavedra (1990), Granite plutonism of the Sierras Pampeanas; an inner cordilleran Paleozoic arc in the southern Andes, *Spec. Pap. Geol. Soc. Am.*, *241*, 77–90.
Rapela, C. W., B. Coira, A. Toselli, and J. Saavedra (1992), The lower Paleozoic magmatism of southwestern Gondwana and the evolution of the Famatinian Orogen, *Int. Geol. Rev.*, *34*, 1081–1142, doi:10.1080/00206819209465657.
Reiners, P. W. (2009), Nonmonotonic thermal histories and contrasting kinetics of multiple thermochronometers, *Geochim. Cosmochim. Acta*, *73*, 3612–3629, doi:10.1016/j.gca.2009.03.038.
Reutter, K. J., E. Scheuber, and D. Helmcke (1991), Structural evidence of orogen-parallel strike slip displacements in the Precordillera of northern Chile, *Geol. Rundsch.*, *80*(1), 135–153, doi:10.1007/BF01828772.
Riller, U., and O. Oncken (2003), Growth of the central Andean Plateau by tectonic segmentation is controlled by the gradient in crustal shortening, *J. Geol.*, *111*(3), 367–384, doi:10.1086/373974.
Royden, L. (1996), Coupling and decoupling of crust and mantle in convergent orogens: Implications for strain partitioning in the crust, *J. Geophys. Res.*, *101*(B8), 17,679–17,705.
Salfity, J. A. (1982), Evolución paleogeográfica del Grupo Salta (Cretácico-Eogénico), Argentina, paper presented at Congreso Latinoamaricano de Geología, Asoc. Geol. Argent., Buenos Aires.
Salfity, J. A. (1985), Lineamientos transversales al rumbo Andino en el noroeste Argentino, paper presented at IV Congreso Geologico Chileno, Asoc. Geol. Chile, Antofagasta, Chile.
Salfity, J. A., and R. A. Marquillas (1994), Tectonic and sedimentary evolution of the Cretaceous-Eocene Salta Group Basin, Argentina, in *Cretaceous Tectonics of the Andes*, edited by J. A. Salfity, pp. 266–315, Vieweg, Brunswick, Germany.
Schildgen, T. F., D. Cosentino, A. Caruso, R. Buchwaldt, C. Yildirim, S. A. Bowring, B. Rojay, H. Echtler, and M. R. Strecker (2012), Surface expression of eastern Mediterranean slab dynamics: Neogene topographic and structural evolution of the southwest margin of the central Anatolian Plateau, Turkey, *Tectonics*, *31*, TC2005, doi:10.1029/2011TC003021.
Schoenbohm, L., and M. R. Strecker (2009), Normal faulting along the southern margin of the Puna plateau, northwest Argentina, *Tectonics*, *28*, TC5008, doi:10.1029/2008TC002341.
Siks, B. C., and B. K. Horton (2011), Growth and fragmentation of the Andean foreland basin during eastward advance of fold-thrust deformation, Puna plateau and Eastern Cordillera, northern Argentina, *Tectonics*, *30*, TC6017, doi:10.1029/2011TC002944.
Sims, J. P., T. R. Ireland, A. Camacho, P. Lyons, P. E. Pieters, R. G. Skirrow, P. G. Stuart-Smith, and R. Miró (1998), U-Pb, Th-Pb and Ar-Ar geochronology from the southern Sierras Pampeanas, Argentina: Implications for the Paleozoic tectonic evolution of the western Gondwana margin, *Geol. Soc. Spec. Publ.*, *142*, 259–281, doi:10.1144/GSL.SP.1998.142.01.13.
Springer, M., and A. Förster (1998), Heat-flow density across the central Andean subduction zone, *Tectonophysics*, *291*, 123–139, doi:10.1016/S0040-1951(98)00035-3.
Strecker, M. R., R. N. Alonso, B. Bookhagen, B. Carrapa, G. E. Hilley, E. R. Sobel, and M. H. Trauth (2007), Tectonics and climate of the southern central Andes, *Annu. Rev. Earth Planet. Sci.*, *35*, 747–787, doi:10.1146/annurev.earth.35.031306.140158.
Tassara, A., H.-J. Goetze, S. Schmidt, and R. Hackney (2006), Three-dimensional density model of the Nazca plate and the Andean continental margin, *J. Geophys. Res.*, *111*, B09404, doi:10.1029/2005JB003976.
Troëng, B., H. Claure, L. Oliveira, R. Ballón, and G. Walser (1993), Thematic maps of the mineral resources of Bolivia. Tarija and Villazón sheets, Geol. Surv. of Bolivia, La Paz.
Turner, J. C. M., and V. Méndez (1975), Geologia del sector oriental de los departamentos de Santa Victoria e Iruya, Provincia de Salta, Republica Argentina. Geology of the eastern regions of Santa Victoria and Iruya, Salta, Argentina, *Bol. Acad. Nac. Cienc.*, *51*(1–5), 12–24.
Vanderhaeghe, O. (2012), The thermal-mechanical evolution of crustal orogenic belts at convergent plate boundaries: A reappraisal of the orogenic cycle, *J. Geodyn.*, *56–57*, 124–145, doi:10.1016/j.jog.2011.10.004.
Viramonte, J. G., S. M. Kay, R. Becchio, M. Escayola, and I. Novitski (1999), Cretaceous rift related magmatism in central-western South America, *J. South Am. Earth Sci.*, *12*, 109–121, doi:10.1016/S0895-9811(99)00009-7.
Viramonte, J. M., R. A. Becchio, J. G. Viramonte, M. M. Pimentel, and R. D. Martino (2007), Ordovician igneous and metamorphic units in southeastern Puna: New U-Pb and Sm-Nd data and implications for the evolution of northwestern Argentina, *J. South Am. Earth Sci.*, *24*, 167–183, doi:10.1016/j.jsames.2007.05.005.
Wdowinski, S., and Y. Bock (1994), The evolution of deformation and topography of high elevated plateaus: 2. Application to the central Andes, *J. Geophys. Res.*, *99*(B4), 7121–7130, doi:10.1029/93JB02396.
Wegmann, M. I., U. Riller, F. D. Hongn, J. Glodny, and O. Oncken (2008), Age and kinematics of ductile deformation in the Cerro Durazno area, NW Argentina: Significance for orogenic processes operating at the western margin of Gondwana during Ordovician-Silurian times, *J. South Am. Earth Sci.*, *26*, 78–90, doi:10.1016/j.jsames.2007.12.004.
Whitman, D., B. L. Isacks, and S. M. Kay (1996), Lithospheric structure and along-strike segmentation of the central Andean Plateau: Seismic *Q*, magmatism, flexure, topography and tectonics, *Tectonophysics*, *259*, 29–40, doi:10.1016/0040-1951(95)00130-1.
Zimmermann, U., and H. Bahlburg (2003), Provenance analysis and tectonic setting of the Ordovician clastic deposits in the southern Puna Basin, NW Argentina, *Sedimentology*, *50*(6), 1079–1104, doi:10.1046/j.1365-3091.2003.00595.x.